Natural Resources for Human Health
eISSN: 2583-1194

Original Research

Received 23 May 2026
Revised 25 June 2026
Accepted 18 July 2026

Natural Resources for Human Health 2026, Vol. 6 (8s): 368–395

KEYWORDS:
Aegle marmelos, nonalcoholic fatty liver disease; high-fat diet; fructose; insulin resistance; inflammation; steatosis, hepatic triglyceride

Ameliorative Effects of Aegle Marmelos Extract on Experimentally Induced Non-Alcoholic Fatty Liver Disease in Wistar Rats

Amol Bhalchandra Deore[1], Mohammed Rageeb Mohammed Usman*[1]

[1]Research Scholar, Smt. Sharadchandrika Suresh Patil College of Pharmacy, Chopda, Maharashtra, India-425107
ORCID: 0000-0001-7743-0445
*[1]Department of Pharmacognosy, Smt. Sharadchandrika Suresh Patil College of Pharmacy, Chopda, Maharashtra, India-425107
ORCID: 0000-0002-3281-2471
Corresponding author: Prof. Dr. Mohammed Rageeb Mohammed Usman
Vice Principal cum Professor and HOD
Email id: drrageebpharmacognosy@gmail.com

ABSTRACT:

Objectives: To investigate the hepatoprotective and metabolic effects of a standardized ethanolic extract of Aegle marmelos Corrêa fruit in a high-fat diet and fructose-induced experimental model of nonalcoholic fatty liver disease in Wistar rats.

Methods: Male Wistar rats (150–180 g) were fed an HFD (60% energy from fat, 5.00 kcal/g) with 10% w/v fructose in drinking water for 16 weeks to induce NAFLD. Following 8 weeks of dietary induction, rats received the ethanolic extract of A. marmelos (250 mg/kg, p.o., once daily) for 8 weeks, with pioglitazone (20 mg/kg, p.o.) as the positive control. The extract, obtained by successive Soxhlet extraction (petroleum ether → ethyl acetate → ethanol) of ripe fruit pulp, was standardized by HPLC. Body mass index, body weight, fasting glucose, insulin, HOMA-IR, serum lipids, hepatic triglycerides, liver function parameters, oxidative stress and antioxidant status, pro-inflammatory cytokines, and hepatic histopathology were assessed.

Results: Chronic HFD/fructose administration produced significant metabolic and hepatic abnormalities, including increased body weight (420.0 g vs. 250.0 g at week 16), body mass index, fasting blood glucose (187.5 ± 3.81 mg/dL vs. 97.5 ± 3.81 mg/dL), insulin and HOMA-IR, dyslipidaemia, hepatic triglyceride accumulation, oxidative stress (elevated MDA with depleted SOD, catalase, GSH), elevated cytokines (TNF-α, IL-1β, IL-6), and hepatocellular injury with vacuolar degeneration and inflammatory infiltration (all $p < 0.0001$ vs. normal control). A. marmelos treatment significantly attenuated these abnormalities — reducing body weight (360.0 g), BMI (0.7545 ± 0.0088 vs. 0.8698 ± 0.0120), fasting glucose (162.5 ± 3.81 mg/dL), HOMA-IR, hepatic triglycerides, total cholesterol, triglycerides, and LDL-C while raising HDL-C restored hepatic antioxidant defenses and plasma total protein, suppressed pro-inflammatory cytokines, and returned liver histology to no abnormality detected. HPLC confirmed umbelliferone (39.38 ppm), quercetin (19.48 ppm), and aegeline (18.32 ppm) as marker constituents. Pioglitazone produced greater improvements in several glycaemic and metabolic endpoints.

Natural Resources for Human Health
eISSN: 2583-1194

Conclusions: The standardized ethanolic A. marmelos extract exerted broad metabolic, antioxidant, anti-inflammatory, and hepatoprotective effects in HFD/fructose-induced NAFLD, mediated by the synergistic bioactivity of its marker compounds, supporting further investigation of the extract as a potential adjunctive therapeutic candidate for NAFLD and associated metabolic disorders.

1. INTRODUCTION

Non-alcoholic fatty liver disease has become the most prevalent chronic liver disorder worldwide, encompassing a spectrum that extends from simple hepatic steatosis through non-alcoholic steatohepatitis—defined by hepatocyte injury, lobular inflammation and variable fibrosis—to cirrhosis and hepatocellular carcinoma [1,2]. The disease is closely intertwined with obesity, insulin resistance, dyslipidaemia, type 2 diabetes mellitus and the metabolic syndrome, and is increasingly regarded as the hepatic manifestation of systemic metabolic dysfunction rather than an isolated hepatic entity [1,3,4]. Recent systematic reviews and meta-analyses estimate the global prevalence of NAFLD at approximately 30–32% of the adult population, with an incidence of 47 cases per 1,000 person-years, higher rates in males (40%) than in females (26%), and regional prevalence exceeding 40% in the Americas and South-East Asia; prevalence has risen from 26% in studies published up to 2005 to 38% in studies published from 2016 onwards, with further increases projected by 2030 [5]. Recognising the metabolic basis of the disease, a multisociety Delphi consensus has proposed replacing the term NAFLD with metabolic dysfunction-associated steatotic liver disease, defined by hepatic steatosis together with at least one cardiometabolic risk factor [6]. Population-based data indicate that roughly 99% of patients diagnosed with NAFLD satisfy the MASLD criteria [7].

The pathogenesis of NAFLD is multifactorial and is best described by the "multiple-hit" model, in which insulin resistance promotes excessive triglyceride accumulation within hepatocytes through increased peripheral lipolysis, enhanced hepatic de novo lipogenesis and impaired fatty-acid oxidation [8]. These metabolic perturbations are compounded by parallel processes—mitochondrial dysfunction, oxidative stress, endoplasmic reticulum stress, adipose-tissue dysfunction with aberrant adipokine secretion, and altered gut–liver signalling—that together drive hepatocellular injury, inflammation and fibrogenesis [8]. Oxidative stress occupies a central position in this cascade: clinical and experimental studies consistently demonstrate elevated lipid peroxidation products, depleted glutathione and reduced activities of superoxide dismutase, catalase and glutathione peroxidase in NAFLD [9–11]. Reactive oxygen species and lipid peroxidation activate redox-sensitive transcription factors such as nuclear factor-κB, which upregulates pro-inflammatory cytokines, notably tumour necrosis factor-α and interleukin-6, amplifying hepatocyte damage and recruiting inflammatory cells [8]. In rats fed a high-fat diet, this oxidative–inflammatory imbalance is reflected in increased lipid peroxidation, protein carbonyl formation and increased NADPH oxidase activity [11].

Animal models are indispensable for dissecting NAFLD pathogenesis and for the preclinical evaluation of candidate interventions [12]. The high-fat diet-fed rat recapitulates the principal features of diet-associated human NAFLD, including weight gain, insulin resistance, dyslipidaemia, hepatic steatosis and oxidative stress, and is widely used to model the metabolic consequences of chronic overnutrition [10]. Feeding Wistar rats a high-fat diet induces hepatic steatosis with biochemical and histopathological changes that mirror the early metabolic phase of human disease [13]. Dietary models, however, require prolonged feeding, generally reproduce inflammation and fibrosis only to a limited and variable degree, and cannot fully capture the genetic and clinical heterogeneity of human NAFLD; these limitations must be considered when extrapolating results [12].

Weight reduction through lifestyle modification remains the cornerstone of NAFLD management, yet sustained weight loss is difficult to achieve and maintain [14,15]. At present, no pharmacological agent is licensed specifically for NAFLD or NASH [14]. International guidelines therefore recommend the off-label use of pioglitazone (30–45 mg/day) or vitamin E (800 IU/day) in selected patients with biopsy-proven NASH—pioglitazone preferentially when diabetes coexists and vitamin E in non-diabetic patients—although both agents carry safety and tolerability concerns [14,16]. Numerous investigational drugs targeting steatosis, oxidative stress, inflammation, the gut-liver axis and fibrosis are in clinical development, but cost, adverse-effect profiles and unproven long-term efficacy continue to motivate the search for safe, accessible alternatives, including plant-derived products [12].

Aegle marmelos Corrêa, commonly known as bael or bel, is a tree native to the Indian subcontinent with a long history of use in Ayurvedic, Siddha and Unani systems of medicine [17]. Its leaves, fruit pulp, bark, roots and seeds contain a rich array of phytochemicals, including flavonoids (rutin, kaempferol-3-*O*-rutinoside), phenolic acids, alkaloids (aegeline, aegelin, shahidine),

coumarins (marmelosin, marmesin, imperatorin, psoralen) and terpenoids [18,19], among which coumarins and flavonoids—particularly marmelosin and rutin—have been reported among its bioactive constituents [18].

A substantial body of preclinical evidence documents antihyperlipidaemic, antidiabetic, antioxidant, anti-inflammatory and hepatoprotective activities of *A. marmelos* extracts [20–26]. In hyperlipidaemic rats, ethanolic leaf extract (125 and 250 mg/kg) significantly reduced serum total cholesterol and triglycerides and raised HDL-cholesterol in Triton WR-1339- and HFD-induced models, with effects comparable to gemfibrozil [27,28], while aqueous leaf and fruit extracts lowered serum and tissue lipids in streptozotocin-induced diabetic rats [29–31]. Antihyperglycaemic mechanisms include enhanced insulin secretion, α-amylase inhibition and retardation of intestinal glucose absorption [32,33]. Directly relevant to NAFLD pathophysiology, a rutin-standardised hydroalcoholic leaf extract attenuated fructose-induced hepatic insulin resistance in rats—improving downstream insulin signalling and modulating hepatic AMPK, SREBP-1c and FoxO1 [34]—and modulated PI3K/STAT-3/mTOR signalling in HepG2 cells [21]. Hepatoprotective effects have been reported against carbon tetrachloride- and cisplatin-induced hepatic injury, with restoration of antioxidant defences and improvement of hepatic histopathology [19,35]. Most recently, marmelosin (the principal coumarin; 99.32% purity) improved glycaemia, insulin resistance, lipid profile, antioxidant status and inflammatory cytokines (TNF-α, IL-1β, IL-6) in HFD- and streptozotocin-induced diabetic rats [36], and aqueous leaf extract attenuated HFD-induced weight gain, dyslipidaemia, hyperleptinaemia and liver-enzyme elevation in obese rats [37]. It must be emphasised, however, that efficacy in these models—which do not replicate the full NAFLD phenotype—does not by itself establish efficacy against HFD-induced NAFLD.

Despite this body of evidence, the specific effect of *A. marmelos* on chronic, diet-induced NAFLD remains inadequately characterised. Earlier hepatoprotective studies relied predominantly on chemical hepatotoxins such as carbon tetrachloride or paracetamol, whose acute mechanisms of hepatocellular necrosis differ fundamentally from the metabolic injury of NAFLD [38], [39], and studies in HFD-fed rats largely focused on body weight and serum lipids without comprehensive assessment of hepatic oxidative stress, steatohepatitis histopathology or lipid-metabolism markers [37]. Because the antioxidant, anti-inflammatory, insulin-sensitising and lipid-lowering properties of *A. marmelos* map directly onto the principal pathogenic drivers of HFD-induced hepatic injury, evaluation of a phytochemically characterised extract in an HFD-fed Wistar rat model is scientifically well founded [27,34,36].

Accordingly, the present study was designed to investigate the ameliorative effect of *Aegle marmelos* extract on high-fat diet-induced NAFLD in Wistar rats. Our hypothesis is that treatment with the extract may attenuate HFD-associated hepatic steatosis and the accompanying biochemical and oxidative disturbances, in a manner consistent with its established antioxidant, anti-inflammatory, insulin-sensitizing and lipid-lowering activities [40].

2. MATERIALS AND METHODS

Chemicals and Reagents

The reagent kits for rat tumor necrosis factor-alpha (TNF-α GENLISA™ ELISA), rat interleukin-1β (IL-1β GENLISA™ ELISA), rat interleukin-6 (IL-6 GENLISA™ ELISA), and rat insulin (INS GENLISA™ ELISA) were purchased from Krishgen Biosystems Private Limited. The triglyceride, direct LDL cholesterol, Alanine Aminotransferase (ALT), Aspartate Aminotransferase (AST), Alkaline Phosphatase (ALP), and glucose reagent kits were purchased from Transasia Bio-Medicals Ltd. (Erba Mannheim); the total cholesterol and total protein reagent kits were purchased from ARKRAY Healthcare Pvt. Ltd.; the direct HDL-C reagent kit was purchased from Pathozyme Diagnostics. The high-fat diet (VRKHFD 60) and normal chow pellet diet were purchased from VRK Nutritional Solutions, Pune, Maharashtra. Pioglitazone hydrochloride was procured from Dr. Reddy's Laboratories. Marker compounds aegeline, quercetin and umbelliferone were purchased from Yucca Enterprises, Mumbai.

Plant Material and Extraction

Healthy, ripe fruits of *Aegle marmelos* were collected from local areas of Nashik, Maharashtra, during the winter season. The plant material was authenticated by the Western Regional Centre, Botanical Survey of India (BSI), Pune, and a voucher specimen (BSI/WRC/Tech./2025/ PSB-110/ Specimen No. 02) was deposited in the herbarium of the Western Regional Centre, Botanical Survey of India, Pune.

The collected ripe fruits were thoroughly washed under running tap water, followed by rinsing with distilled water to remove adhering dirt, soil, and surface impurities. The hard outer shell (pericarp) was carefully cracked open, and the fruit pulp, along

with the rind, was separated (seeds were removed). The fruit pulp was cut into small uniform pieces and shade-dried at room temperature (and subsequently dried in a hot air oven at a controlled temperature of 40–45°C) until completely dehydrated to a constant weight. The dried fruit material was pulverized into a coarse, uniform powder using an electric mixer grinder. Approximately 500 g of dried fruit powder was obtained and stored in clean, airtight glass containers at room temperature, protected from direct sunlight, until further extraction.

For successive Soxhlet extraction, approximately 200 g of the dried, powdered ripe fruit material of *Aegle marmelos* was accurately weighed, uniformly packed into a cellulose extraction thimble, and placed into the Soxhlet extraction chamber. The apparatus was fitted with a 500 mL round-bottom flask containing approximately 350–400 mL of the respective solvent. Successive extraction was carried out using solvents in increasing order of polarity: petroleum ether, ethyl acetate, and ethanol. The powdered fruit material was first extracted with petroleum ether for approximately 18–24 h, or until the solvent in the siphoning chamber became clear and colorless. After completion of this step, the plant residue (marc) was separated and thoroughly air-dried at room temperature to remove residual non-polar solvent before proceeding to the next solvent.

The dried marc was subsequently extracted with 350–400 mL of ethyl acetate for approximately 18–24 h under continuous Soxhlet extraction. Upon completion, the residue was again air-dried and subjected to extraction with 350–400 mL of ethanol for approximately 18–24 h. The successive use of petroleum ether, ethyl acetate, and ethanol facilitated the systematic extraction of non-polar (lipids/fatty acids), moderately polar, and polar phytoconstituents (alkaloids, flavonoids, tannins, and carbohydrates/pectins), respectively [41]. This solvent sequence is consistent with the reported phytochemistry of *A. marmelos* fruit, whose pulp is rich in bioactive substances including phenolics, alkaloids, pectins, tannins, coumarins, flavonoids, and terpenoids, with reducing sugars and carotenoids also documented in the fruit [42].

Each solvent extract obtained after Soxhlet extraction was filtered through Whatman No. 1 filter paper to remove residual particulate matter. The filtrates were concentrated under reduced pressure using a rotary evaporator at a controlled temperature of 40–45°C to prevent thermal degradation of thermolabile constituents. The concentrated extracts were further dried to obtain the respective crude extracts. Each dried extract was accurately weighed, and the percentage yield was calculated relative to the initial dry powder weight. Successive Soxhlet extraction of 200 g of powdered ripe fruits of *Aegle marmelos* yielded petroleum ether, ethyl acetate, and ethanolic extracts in quantities of 4.80 g (2.40% w/w), 8.40 g (4.20% w/w), and 19.60 g (9.80% w/w), respectively.

Ethanol demonstrated the highest extraction efficiency for the fruit matrix compared to methanol and aqueous solvents [43]. All crude extracts were separately transferred into clean, airtight glass containers, labeled appropriately, and stored at 2–8°C, protected from direct light, moisture, and contamination until further phytochemical screening and biological evaluation.

HPLC Analysis

The *Aegle marmelos* extract was standardized by HPLC using aegeline, quercetin, and umbelliferone as marker compounds, three constituents with established biological relevance to the extract's anticipated hepatometabolic activity [44]. . Analysis was performed on an HPLC 3000 Series system equipped with a binary-gradient pump (P-3000M), UV-3000M detector, manual injector, and HPLC Workstation software. Separation was achieved on a Cosmosil C18 column (250 × 4.6 mm, 5 μm) using methanol:water (70:30, v/v) as the mobile phase at a flow rate of 0.8 mL/min. The injection volume was 20 μL.

Aegeline, quercetin, and umbelliferone were detected at 223, 256, and 216 nm, respectively, while the extract was analyzed at 214 nm. Standard stock solutions (1000 ppm) were prepared by dissolving 10 mg of each standard in 10 mL of mobile phase. Working standards were prepared at 50 ppm by diluting 0.5 mL stock solution to 10 mL.

The extract sample was dissolved in methanol:water (70:30), sonicated, diluted to the required concentration, and filtered before injection. Quantification was performed by comparing sample and standard peak areas. This approach follows established analytical practice for *A. marmelos*, in which reversed-phase chromatographic methods using coumarin and flavonoid markers have been developed and validated for quantitative analysis and quality control of bael fruit extracts and polyherbal formulations [44,45].

Table 1: Quantitative Analysis of Selected Marker Compounds in the *A. marmelos* ethanolic extract

Marker	Standard area	Sample area	Concentration
Aegeline	1,512,529	554,239	18.32 ppm
Umbelliferone	1,140,515	898,181	39.38 ppm
Quercetin	1,134,089	441,875	19.48 ppm

Animal Models and Experimental Design

Wistar rats of either sex, weighing 150–180 g, were used for the in vivo study. The Wistar strain is among the most widely employed outbred rat models in nutritional and hepatobiliary research, with strain, diet composition, and feeding period all recognized as determinants of NAFLD development in this species [46]. A total of 24 animals were included and acclimatized for one week before initiation of the experiment. The animals were housed under standard laboratory conditions at 25 ± 0.5 °C with a 12:12 h light–dark cycle and had free access to food and water, except where otherwise specified.

All experimental procedures were performed in accordance with the guidelines of the Committee for the Control and Supervision of Experiments on Animals, Government of India, and were approved by the Institutional Animal Ethics Committee under approval no. IAEC/CPD/415/11. The study was conducted at the Animal House of Smt. Sharadchandrika Suresh Patil College of Pharmacy, Chopda, Jalgaon, Maharashtra, India (registration no. 316/PO/ReBi/S/2000/CPCSEA, dated 02/11/2022).

Following acclimatization, the animals were divided into four groups (n = 6/group). The normal control group received standard laboratory chow (3.365 kcal/g; VRK Nutritional Solutions, Pune, India), whereas the remaining groups received a high-fat diet (VRKHFD 60; VRK Nutritional Solutions, Pune, India) providing 60% of energy from fat, 25.6% from carbohydrate, and 14.4% from protein, with an estimated energy content of 5.00 kcal/g. High-fat diets of this composition are well established to induce obesity, dyslipidemia, insulin resistance, and hepatic steatosis in rodents over extended feeding periods [13]. The diets contained appropriate vitamin and mineral mixtures. Animals in the HFD groups also received 10% w/v fructose in drinking water continuously from Day 1 until the end of week 16; co-administration of fructose with high saturated fat synergistically accelerates hepatic *de novo* lipogenesis and insulin resistance [47], and such combined diets produce rodent hepatic phenotypes most closely resembling human NAFLD [48].

After 8 weeks of dietary induction, treatment was initiated and continued for 8 weeks (weeks 9–16). The experimental groups and treatment schedule are presented in Table 2.

Table 2. Experimental design and treatment schedule

Group	Experimental group	Dietary regimen and treatment	Dose and route	Treatment period
I	Normal Control (ND)	Normal chow diet + 0.5% CMC	10 mL/kg, p.o.	Weeks 1–16
II	Disease Control (HFD)	HFD + 10% w/v fructose in drinking water	—	Weeks 1–16
III	*Aegle marmelos* Extract (AME250)	HFD + 10% w/v fructose in drinking water + ethanolic extract of *A. marmelos*	250 mg/kg, p.o.	Weeks 9–16
IV	Positive Control (PIO20)	HFD + 10% w/v fructose in drinking water + pioglitazone HCl	20 mg/kg, p.o.	Weeks 9–16

The ethanolic extract of *Aegle marmelos* and pioglitazone hydrochloride were separately suspended in 0.5% CMC prepared in distilled water immediately before administration. The respective treatments were administered once daily by oral gavage from weeks 9–16. The normal-control group received 0.5% CMC as the vehicle at a volume of 10 mL/kg body weight, p.o. Body

weight, food intake, and water consumption were monitored weekly throughout the experimental period to assess the metabolic impact of the intervention.

The disease-control group received the HFD and 10% w/v fructose in drinking water throughout the 16-week experimental period without receiving any test treatment. The fructose solution was supplied through drinking-water bottles and was not administered by oral gavage.

Food intake, body weight, naso-anal length, body mass index, and fasting blood glucose were assessed at predetermined time points, i.e., at the end of weeks 1, 8, and 16. Longitudinal recording of feed intake and body weight indices alongside glycemic measurements follows established practice in dietary rodent studies of obesity and NAFLD [49], and fasting blood glucose assessment in these models is routinely performed using tail-tip capillary blood sampling [50].

Blood Collection, Plasma Separation, and Biochemical Analysis

After 16 weeks, Wistar rats were fasted for 8–12 h and anesthetized with isoflurane. Blood was collected from the dorsal aorta using EDTA-containing Vacutainer tubes. Samples were centrifuged at 3,000 × g for 15 min at 25 °C, and the separated plasma was stored at 2–8 °C until analysis.

Plasma was analyzed for fasting glucose and insulin to calculate HOMA-IR, along with liver function markers (albumin, total protein, bilirubin, ALT, AST, and ALP) and lipid profile parameters (triglycerides, total cholesterol, HDL, and LDL). All analyses were performed using commercial diagnostic kits on an ERBA XL-180 automated clinical chemistry analyzer.

Absolute Liver Weight and Hepatosomatic index

At the end of the experimental period, the animals were euthanized according to the approved animal ethics protocol. The liver was excised, washed with ice-cold PBS (pH 7.4), blotted dry, and weighed immediately. Relative liver weight (hepatosomatic index) was calculated as a percentage of the final body weight using the formula: hepatosomatic index (%) = (Absolute liver weight ÷ final body weight) × 100 [51]. This endpoint is widely used as an index of diet-induced hepatic lipid accumulation, as hepatomegaly and increased liver mass are characteristic consequences of high-fat feeding and correlate with hepatic triglyceride deposition [52].

Tissue Homogenate Preparation

Liver tissues were collected after euthanasia, rinsed with ice-cold PBS (pH 7.4), and homogenized in chilled PBS containing protease inhibitors to prepare a 10% (w/v) homogenate. Homogenates were centrifuged at 10,000 × g for 15 min at 4 °C, and the supernatants were collected, aliquoted, and stored at −80 °C until analysis. Samples were diluted as required and equilibrated to room temperature before testing. Standards and samples were analyzed in duplicate.

The supernatants were assessed for antioxidant markers (total protein, CAT, SOD, GSH, and lipid peroxidation) and inflammatory cytokines (IL-1β, IL-6, and TNF-α). Preparation of hepatic homogenates in ice-cold phosphate buffer for downstream antioxidant analysis follows established methodology in high-fat diet rat studies [53], and the quantification of hepatic TNF-α, IL-1β, IL-6, MDA, and SOD in tissue homogenates by ELISA and commercial assay kits is consistent with prior protocols used in hepatometabolic rodent models [54].

Homeostatic Model Assessment of Insulin Resistance

Insulin resistance was assessed using the Homeostatic Model Assessment of Insulin Resistance (HOMA-IR). Following a 12-h fasting period, fasting blood samples were collected and plasma glucose and insulin concentrations were determined. Fasting glucose was estimated using the GOD-POD method[55], while plasma insulin was measured using the Rat Insulin GENLISA™ ELISA kit. HOMA-IR was calculated from fasting glucose and insulin concentrations according to the equation described by Matthews et al. (1985). Higher HOMA-IR values indicated greater insulin resistance [56]. Specifically, the index was derived using the formula: [fasting insulin (μU/mL) × fasting glucose (mg/dL)] / 405 [57].

Antioxidant activity

Estimation of Catalase

Catalase activity was estimated spectrophotometrically according to Aebi [58], based on the decomposition of hydrogen peroxide (H_2O_2) into water and oxygen. The decrease in absorbance at 240 nm was monitored for 3 min at 1-min intervals.

The reaction mixture contained 3.0 mL of 30 mM H_2O_2, 0.5 mL of 50 mM phosphate buffer (pH 7.0), and 0.5 mL of supernatant from a 10% tissue homogenate. Catalase activity was calculated from the rate of decrease in absorbance using the molar extinction coefficient of H_2O_2 ($\varepsilon = 43.6\ M^{-1}\ cm^{-1}$) and expressed as μmol H_2O_2 decomposed/min/mg protein.

Estimation of Superoxide Dismutase (SOD)

Superoxide dismutase activity was estimated by the method of Kono (1978), based on the inhibition of nitroblue tetrazolium (NBT) reduction by superoxide radicals generated from hydroxylamine autoxidation [59]. The reaction mixture contained sodium carbonate buffer (50 mM, pH 10.2), EDTA (0.1 mM), NBT (24 μM), hydroxylamine hydrochloride (1 mM), Triton X-100 (0.03%), and tissue homogenate. The mixture was incubated at 37°C for 20 min, and absorbance was measured at 560 nm against a reagent blank.

SOD activity was determined from the percentage inhibition of NBT reduction relative to the control. One unit of SOD was defined as the amount of enzyme producing 50% inhibition under the assay conditions. Activity was expressed as U/mL homogenate and, where applicable, U/mg protein.

Estimation of Reduced Glutathione (GSH)

Reduced glutathione (GSH) was estimated by the method of Moron et al. (1979), based on the reaction of GSH sulfhydryl groups with 5,5'-dithiobis-(2-nitrobenzoic acid) (DTNB) to form a yellow-colored product, measured at 412 nm [60]. Briefly, 0.5 mL of supernatant from a 10% tissue homogenate was deproteinized with 0.5 mL of 4% sulfosalicylic acid, followed by addition of 4.0 mL of 0.01 M DTNB prepared in PBS (pH 7.4). Absorbance was measured at 412 nm against a reagent blank using a UV–Visible spectrophotometer.

GSH concentration was calculated from the absorbance and expressed as μmol/mL of tissue homogenate. Where required, GSH levels were normalized to the protein concentration determined using a BSA standard curve and expressed as μmol/mg protein.

Estimation of Lipid Peroxidation (LPO)

Lipid peroxidation was estimated by the thiobarbituric acid reactive substances (TBARS) method described by Ohkawa et al. (1979). The assay is based on the reaction of malondialdehyde (MDA), a lipid peroxidation product, with thiobarbituric acid (TBA) to form a pink-colored MDA–TBA complex, measured at 532 nm [61].

Briefly, 0.1 mL of 10% tissue homogenate was mixed with 0.2 mL of 8% sodium lauryl sulfate, 1.5 mL of 20% acetic acid (pH 3.5), and 1.5 mL of 0.8% TBA. The mixture was heated at 95°C for 60 min, cooled, extracted with n-butanol:pyridine (15:1), and centrifuged at 2200 × g for 5 min. The absorbance of the organic layer was measured at 532 nm against a reagent blank.

MDA concentration was calculated using the molar extinction coefficient of the MDA–TBA complex ($1.56 \times 10^5\ M^{-1}\ cm^{-1}$) and expressed as nmol MDA/mL tissue homogenate. LPO was also normalized to protein concentration and expressed as nmol MDA/mg protein.

Estimation of Hepatic Triglyceride

Hepatic triglyceride (TG) content was determined using a direct colorimetric method adapted from Butler et al. (1961). Briefly, liver tissue was homogenized in nine volumes of phosphate buffer (M/15, pH 7.0) for 90 s. A 1-mL aliquot of the homogenate was mixed with activated silica gel and chloroform and shaken intermittently for 10 min. Phospholipids were adsorbed onto the silica gel, while triglycerides were extracted into the chloroform phase. The extract was filtered, and an aliquot containing approximately 0.05 mg of triglycerides was used for analysis. Corn oil (0.05 mg/mL) served as the standard. The chloroform was evaporated, followed by saponification with alcoholic potassium hydroxide. After acidification with sulfuric acid, glycerol released from triglyceride hydrolysis was oxidized with sodium periodate to form formaldehyde. The formaldehyde was subsequently reacted with chromotropic acid to produce a colored complex. Absorbance was measured spectrophotometrically at 570 nm [62].

Hepatic TG concentration was calculated from the corrected absorbance ratio of the sample to the corn-oil standard and expressed as mg/g tissue:

Natural Resources for Human Health
eISSN: 2583-1194

$$Hepatic\ TG\ \left(\frac{mg}{g}tissue\right) = \frac{10}{A}\left[\frac{OD_{SU} - OD_{UU}}{OD_{SS} - OD_{US}}\right]$$

where A is the volume (mL) of the chloroform extract aliquot used for analysis, and OD_{SU}, OD_{UU}, OD_{SS}, and OD_{US} represent the absorbance values of the saponified unknown, unsaponified unknown, saponified standard, and unsaponified standard, respectively.

Histopathological Study

Following euthanasia, the intact livers were excised, rinsed with normal saline, dried on filter paper, weighed, and grossly examined. Representative tissue samples from the right hepatic lobes were fixed in 10% formalin for 24 h, dehydrated through graded ethanol, cleared in xylene, embedded in paraffin, sectioned at 3–5 µm, and stained with hematoxylin and eosin (H&E). Histological features of the treatment groups were compared with those of the control group [63,64].

Steatosis and hepatocellular hypertrophy were evaluated microscopically at 40× magnification. Lesions were graded based on the percentage of tissue affected as follows: 0 = no abnormality detected/within normal limits, 1 = minimal (0–10%), 2 = mild (11–20%), 3 = moderate (21–40%), and 4 = severe (41–100%). Lesions were further characterized according to their organ-specific topography, distribution (focal, multifocal, or diffuse), nature, and duration [63].

Statistical Analysis

Data were expressed as the mean ± standard error of the mean. Differences among experimental groups were analysed using a one-way analysis of variance followed by Tukey's post-hoc test for multiple group comparisons. Differences between groups were considered statistically significant at a threshold of $p < 0.05$. GraphPad Prism 11.1.0 software was used for all statistical calculations and the generation of graphical representations.

3. RESULTS

HPLC Analysis of *Aegle marmelos* Extract and Marker Compounds

To standardize the ethanolic extract dried fruits of *Aegle marmelos* and quantify key phytoconstituents relevant to its biological activity, a reversed-phase HPLC-UV method was utilized. Isocratic separation on a Cosmosil C18 column (250 × 4.6 mm, 5 µm) using methanol:water (70:30, v/v) at 0.8 mL/min successfully resolved three major phytochemical markers: umbelliferone, quercetin, and aegeline. Chromatographic identification was confirmed by matching retention times with reference standards under identical analytical conditions. In the *A. marmelos* extract chromatogram, umbelliferone eluted at $t_R \approx 4.240$ min, quercetin at $t_R \approx 5.268$ min, and aegeline at $t_R \approx 6.039$ min, aligning closely with the pure standard peaks at $t_R \approx 4.323$ min, 5.416 min, and 6.390min, respectively. Quantitative evaluation via peak area integration revealed that umbelliferone was present as the predominant bioactive constituent at a concentration of 39.38 ppm (sample peak area: 898,181), followed by quercetin at 19.48 ppm (sample peak area: 441,875) and aegeline at 18.32 ppm (sample peak area: 554,239).

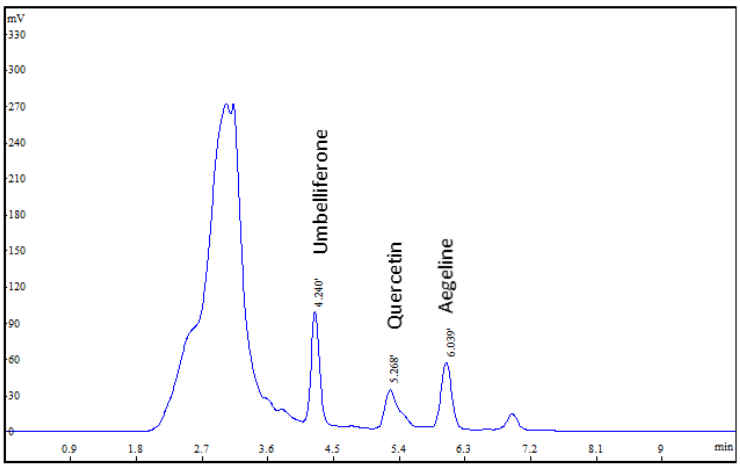

Figure 1. Reversed-phase HPLC chromatographic profiling of *Aegle marmelos* ethanolic extract

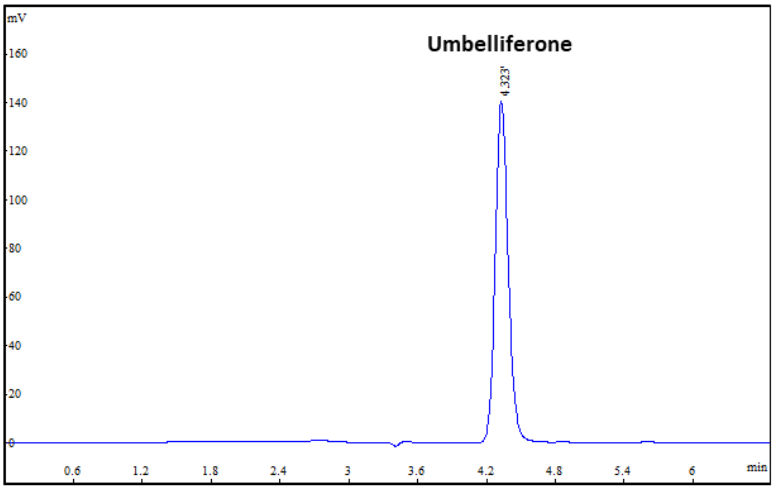

Figure 2. Reversed-phase HPLC chromatogram of the umbelliferone standard

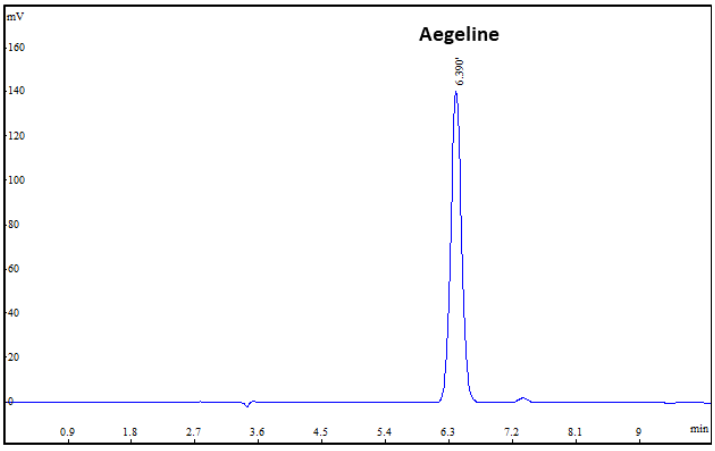

Figure 3. Reversed-phase HPLC chromatogram of the aegeline standard

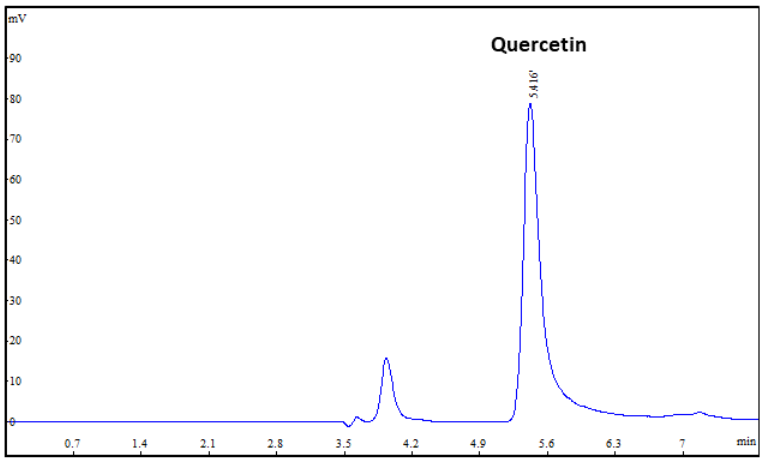

Figure 4. Reversed-phase HPLC chromatogram of the quercetin standard

Natural Resources for Human Health
eISSN: 2583-1194

Effect of *Aegle marmelos* extract on Food Intake on animals fed on HFD and fructose

To evaluate the effect of high-fat diet (HFD) combined with fructose and subsequent treatment with *Aegle marmelos* extract (AME250, 250 mg/kg p.o.) or pioglitazone (PIO20, 20 mg/kg p.o.) on dietary behavior, daily food intake (g/day/rat) was quantified at Weeks 1, 8, and 16. Rats receiving a standard normal diet (ND) consumed significantly greater amounts of food compared to the HFD-fed groups at all analyzed time points (Week 1: $p < 0.0001$; Week 8: $p < 0.0001$; Week 16: $p < 0.0001$). Similarly, significant differences were sustained when comparing ND to AME250 ($p < 0.001$ at W1; $p < 0.0001$ at W8 and W16) and ND to PIO20 ($p < 0.01$ at W1; $p < 0.0001$ at W8 and W16). Intervention with either AME250 or PIO20 from Weeks 9 to 16 caused no significant alteration in food intake compared to the HFD disease-control group ($p > 0.05$). Furthermore, no significant differences in food intake were recorded between the AME250 and PIO20 treatment groups at any time point ($p > 0.05$).

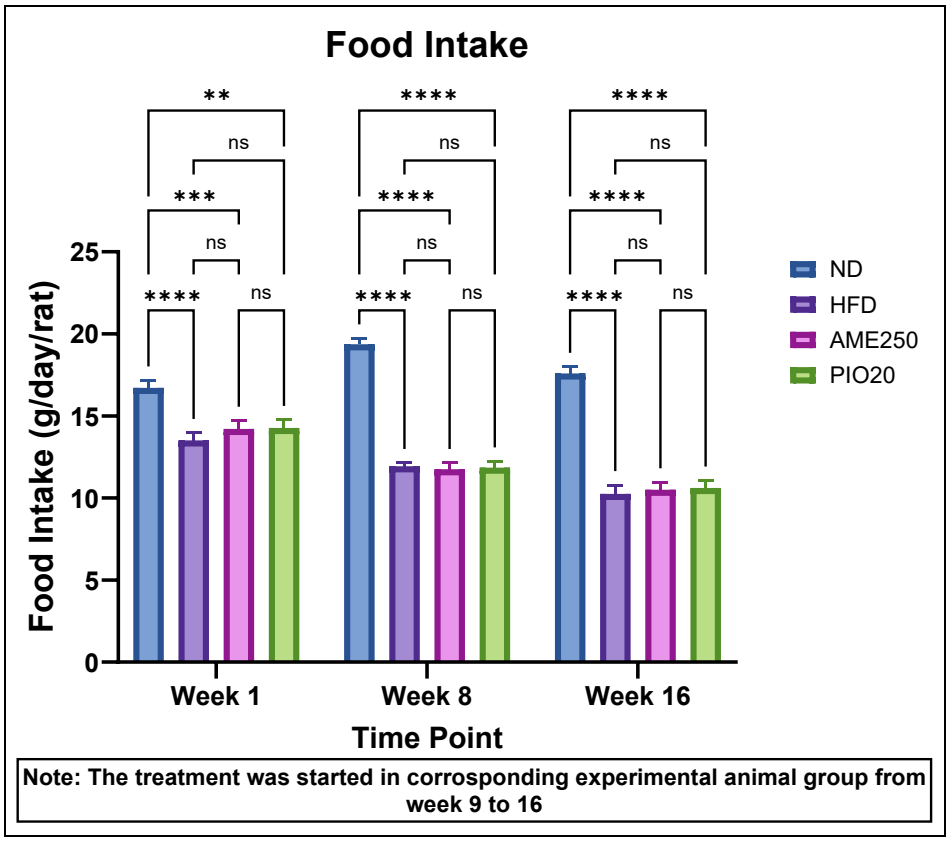

Figure 5. Effect of *Aegle marmelos* extract on food intake in HFD and fructose induced NAFLD in Wistar rats at different time points. Food intake (g/day/rat) was recorded in normal diet control (ND), high-fat diet + 10% fructose disease control (HFD), *Aegle marmelos* extract-treated (AME250, 250 mg/kg p.o.), and pioglitazone-treated (PIO20, 20 mg/kg p.o.) Wistar rats. Treatments were administered daily from Week 9 to Week 16. Data are presented as Mean ± SEM. Statistical analysis was performed using ordinary two-way ANOVA followed by Tukey's multiple-comparisons test. *$p < 0.05$,* *p < 0.01, *** p < 0.001, **** p < 0.0001, and ns = non-significant ($p > 0.05$).

Effect of *Aegle marmelos* extract on Body Weight and Body Mass Index on animals fed on HFD and fructose

To determine the impact of high-fat diet (HFD) plus fructose induction and subsequent therapeutic intervention on physical anthropometric parameters, body weight (BW) and body mass index (BMI) were measured at Weeks 1, 8, and 16. Baseline baseline measurements at Week 1 showed no statistically significant differences across any experimental groups for either parameter ($p > 0.05$). Continuous administration of HFD and 10% fructose water for 8 weeks resulted in a marked escalation in both body weight and BMI in all high-fat diet groups compared to normal diet controls (ND vs HFD, ND vs AME250, ND vs PIO20: $p < 0.0001$ for BW; $p < 0.01$ to $p < 0.0001$ for BMI). Following the intervention phase (Weeks 9–16), the HFD disease control group displayed further increases in body weight (~420 g) and BMI (~0.86 kg/m²), remaining significantly

elevated relative to ND controls ($p < 0.0001$). Treatment with *Aegle marmelos* extract (AME250) or pioglitazone (PIO20) from Weeks 9 to 16 significantly mitigated HFD-induced gains in both body weight and BMI compared to the untreated HFD control group ($p < 0.0001$). Furthermore, pioglitazone exhibited a significantly greater reduction in both BW and BMI compared to AME250 at Week 16 ($p < 0.0001$).

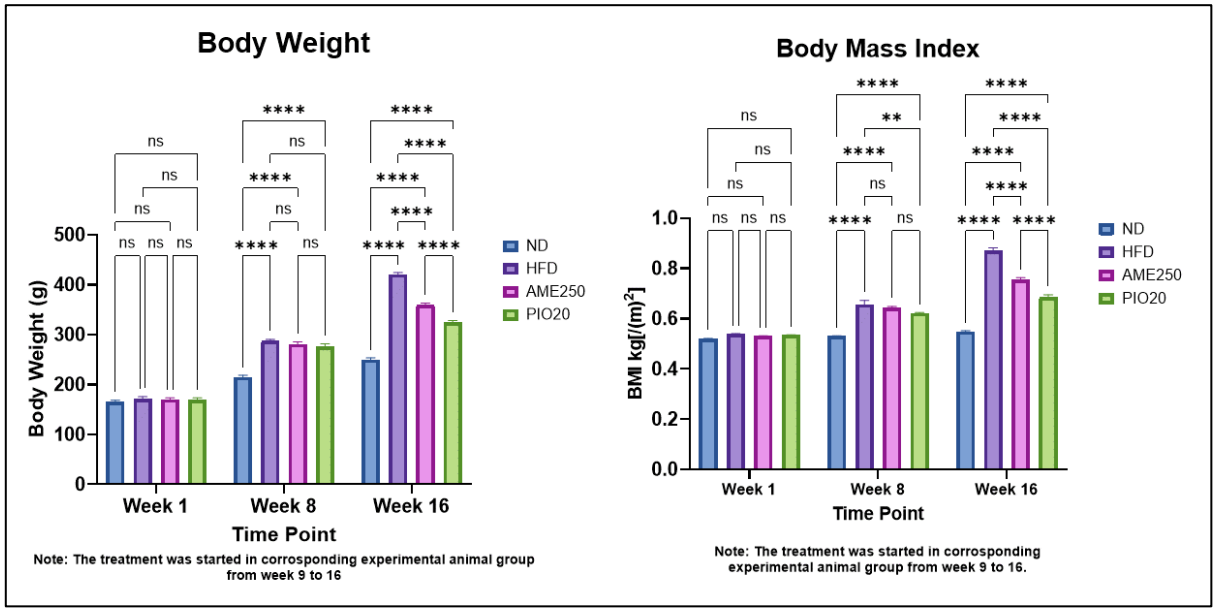

Figure 6. Effect of *Aegle marmelos* extract on body weight and body mass index in HFD and fructose induced NAFLD in Wistar rats at different time points**.** Progression of (**A**) Body Weight (g) and (**B**) Body Mass Index (kg/m^2) across experimental groups at Weeks 1, 8, and 16. Groups: Normal Diet control (ND), High-Fat Diet + 10% Fructose disease control (HFD), *Aegle marmelos* extract (AME250, 250 mg/kg p.o.), and Pioglitazone (PIO20, 20 mg/kg p.o.). Treatments were administered daily from Week 9 through Week 16. Values represent Mean ± SEM. Statistical analysis was performed using ordinary two-way ANOVA with Tukey's post-hoc multiple-comparisons test. **p < 0.01,** * $p < 0.001$, **** $p < 0.0001$, ns = non-significant ($p > 0.05$).

Effect of *Aegle marmelos* extract on Fasting Blood Glucose on animals fed on HFD and fructose

Fasting blood glucose (FBG) levels were evaluated at Weeks 1, 8, and 16 to assess glycemic control across experimental groups. Baseline FBG levels at Week 1 were comparable across all groups with no statistically significant differences ($p > 0.05$). Following 8 weeks of dietary induction, all high-fat diet and fructose-fed groups demonstrated a marked, statistically significant elevation in FBG compared to normal diet controls (ND vs. HFD, AME250, and PIO20: $p < 0.0001$), confirming induction of fasting hyperglycemia. By Week 16, the untreated HFD control group exhibited severe hyperglycemia (~188 mg/dL), remaining significantly higher than ND controls ($p < 0.0001$). Daily intervention with *Aegle marmelos* extract (AME250, 250 mg/kg p.o.) from Weeks 9 to 16 significantly reduced fasting blood glucose levels compared to the HFD disease control group ($p < 0.001$). Standard treatment with pioglitazone (PIO20, 20 mg/kg p.o.) produced a further significant attenuation of FBG relative to HFD ($p < 0.0001$). Furthermore, PIO20 demonstrated superior antihyperglycemic efficacy compared to AME250 at Week 16 ($p < 0.01$).

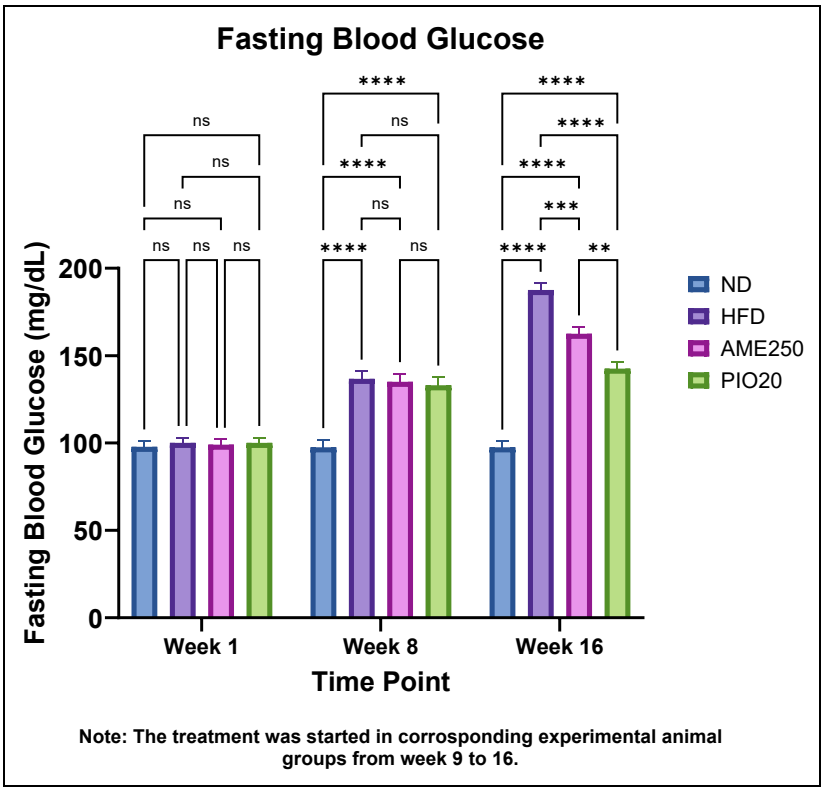

Figure 7. Effect of *Aegle marmelos* extract on fasting blood glucose in HFD and fructose induced NAFLD in Wistar rats at different time points. Fasting blood glucose (mg/dL) measured at Weeks 1, 8, and 16 across experimental groups: Normal Diet control (ND), High-Fat Diet + 10% Fructose disease control (HFD), Aegle marmelos extract (AME250, 250 mg/kg p.o.), and Pioglitazone (PIO20, 20 mg/kg p.o.). Treatments were administered p.o. daily from Week 9 to Week 16. Values represent Mean ± SEM. Statistical analysis was performed using ordinary two-way ANOVA with Tukey's post-hoc test. $p < 0.01$, * $p < 0.001$, **** $p < 0.0001$, ns = non-significant ($p > 0.05$).

Effect of *Aegle marmelos* extract on Insulin and HOMA-IR on animals fed on HFD and fructose

To evaluate the impact of dietary induction and subsequent therapeutic intervention on systemic insulin sensitivity, fasting plasma insulin levels and the Homeostatic Model Assessment of Insulin Resistance (HOMA-IR) index were determined at Week 16. Chronic administration of a high-fat diet combined with 10% fructose water induced marked hyperinsulinemia (~46 µIU/mL) and severe systemic insulin resistance (~21.3) in the HFD disease control group compared to normal diet controls (ND vs HFD: $p < 0.0001$ for both parameters). Treatment with *Aegle marmelos* extract (AME250, 250 mg/kg p.o.) from Weeks 9 to 16 significantly attenuated both fasting insulin concentration (~33 µIU/mL) and HOMA-IR (~13.1) relative to the untreated HFD group ($p < 0.0001$). Standard intervention with pioglitazone (PIO20, 20 mg/kg p.o.) demonstrated a potent restoration of insulin sensitivity, returning both insulin levels (~13.3 µIU/mL) and HOMA-IR values (~4.6) to levels statistically indistinguishable from the normal diet control group (ND vs PIO20: ns, $p > 0.05$). Consequently, pioglitazone achieved a significantly lower fasting insulin and HOMA-IR score compared to AME250 ($p < 0.0001$).

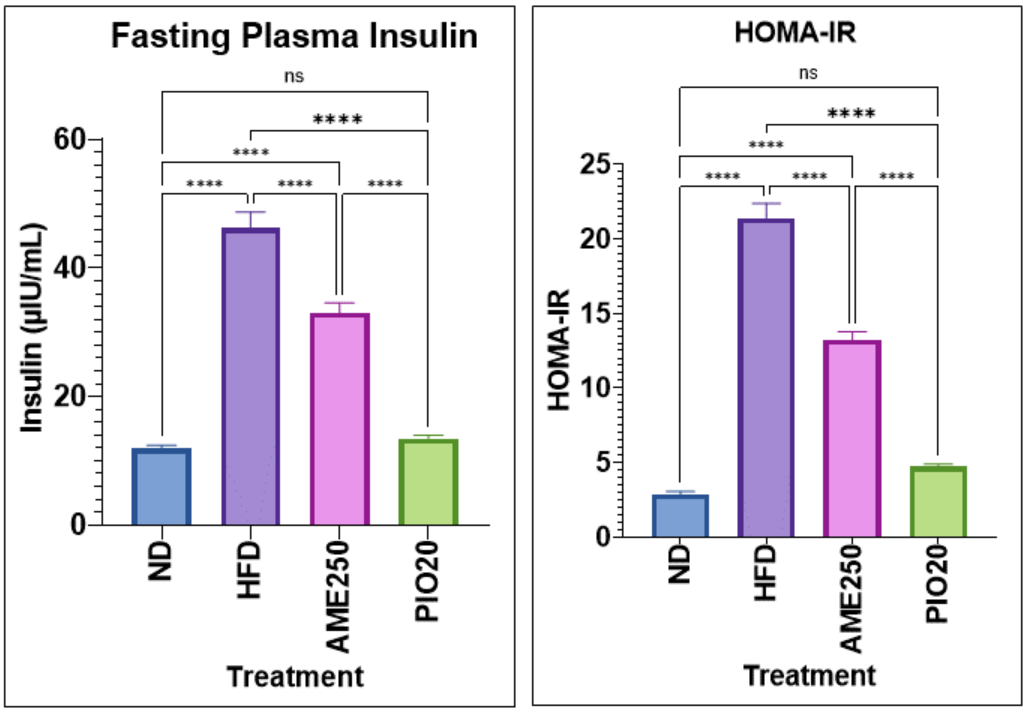

Figure 8. Effect of *Aegle marmelos* extract on fasting plasma insulin levels and HOMA-IR in HFD and fructose induced NAFLD in Wistar rats at week 16. Quantifications of (**A**) Fasting Plasma Insulin (µIU/mL) and (**B**) HOMA-IR score across experimental groups: Normal Diet control (ND), High-Fat Diet + 10% Fructose disease control (HFD), *Aegle marmelos* extract (AME250, 250 mg/kg p.o.), and Pioglitazone (PIO20, 20 mg/kg p.o.). Treatments were administered daily from Week 9 to Week 16. Bars represent Mean ± SEM. Statistical analysis was performed using ordinary one-way ANOVA with Tukey's post-hoc multiple-comparisons test. **** $p < 0.0001$, ns = non-significant ($p > 0.05$).

Effect of *Aegle marmelos* extract on Absolute Liver Weight and Hepato somatic Index on animals fed on HFD and fructose

To determine the impact of dietary induction and oral treatments on organ-level hepatomegaly, absolute liver weight (g) and the hepatosomatic index (HSI, %) were evaluated at Week 16. Chronic consumption of a high-fat diet supplemented with 10% fructose water induced marked hepatomegaly, significantly elevating absolute liver weight (~20.7 g) and HSI (~4.9%) in the untreated HFD group compared to normal diet controls (~9.6 g and ~3.8%, respectively; $p < 0.0001$ for both parameters). Treatment with *Aegle marmelos* extract (AME250, 250 mg/kg p.o.) from Weeks 9 to 16 produced a prominent reduction in both absolute liver weight (~15.8 g) and HSI (~4.4%) compared to the HFD control group ($p < 0.0001$). Standard treatment with pioglitazone (PIO20, 20 mg/kg p.o.) also significantly attenuated absolute liver weight (~13.1 g, $p < 0.0001$) and normalized the HSI (~4.0%) to values that were statistically comparable to the normal diet control group (ND vs PIO20: ns, $p > 0.05$). Comparative evaluation revealed that pioglitazone achieved significantly lower absolute liver weight ($p < 0.001$) and HSI ($p < 0.01$) relative to AME250.

Natural Resources for Human Health
eISSN: 2583-1194

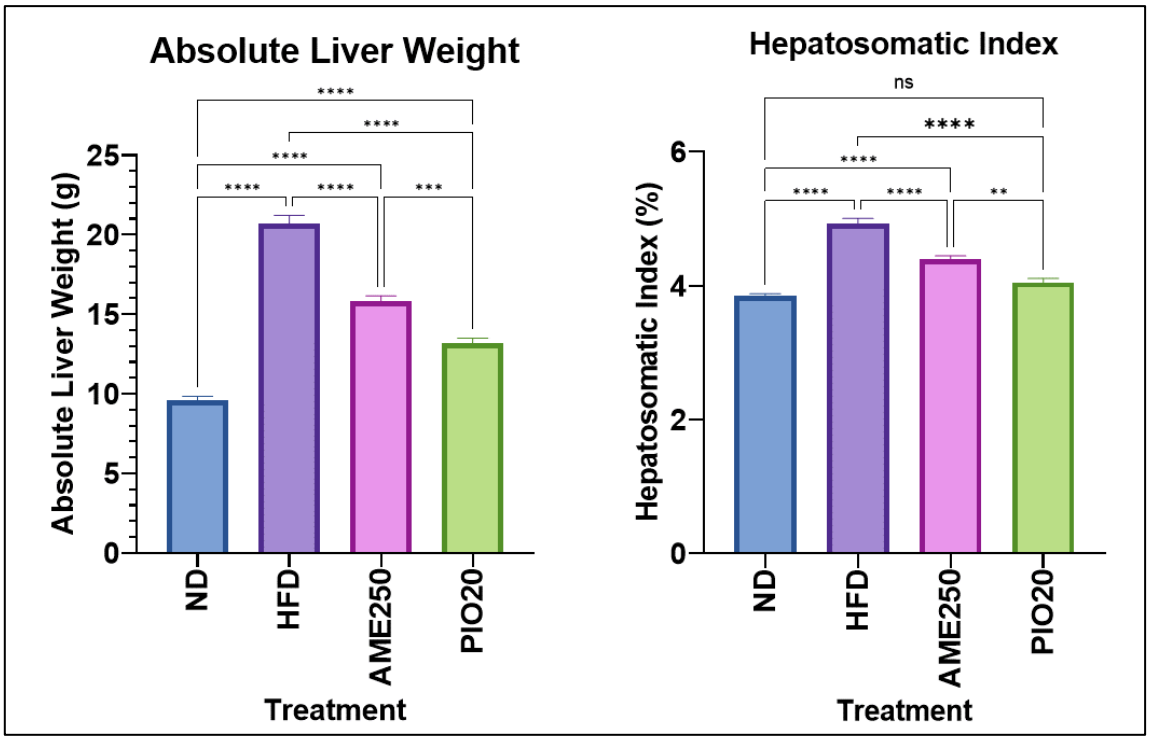

Figure 9. Effect of *Aegle marmelos* extract on absolute liver weight and hepatosomatic index in HFD and fructose induced NAFLD in Wistar rats at week 16. Quantification of (**A**) Absolute Liver Weight (g) and (**B**) Hepatosomatic Index (%) across experimental groups: Normal Diet control (ND), High-Fat Diet + 10% Fructose disease control (HFD), *Aegle marmelos* extract (AME250, 250 mg/kg p.o.), and Pioglitazone (PIO20, 20 mg/kg p.o.). Treatments were administered daily from Week 9 to Week 16. Values represent Mean ± SEM. Statistical analysis was conducted using ordinary one-way ANOVA followed by Tukey's post-hoc test. **$p < 0.01$,** * $p < 0.001$, **** $p < 0.0001$, ns = non-significant ($p > 0.05$).

Effect of *Aegle marmelos* extract on Liver Function Test parameters on animals fed on HFD and fructose

To determine the hepatoprotective efficacy of *Aegle marmelos* extract against HFD- and fructose-induced liver injury, plasma total protein concentrations and serum biomarker enzymes (ALT, AST, and ALP) were evaluated at Week 16. The untreated HFD disease-control group exhibited marked hepatocellular injury, characterized by significant surges in ALT (~143 IU/L), AST (~208 IU/L), and ALP (~300 IU/L) levels alongside a notable reduction in plasma total protein (~5.9 g/dL) compared to normal diet controls (~41 IU/L, ~82 IU/L, ~126 IU/L, and ~6.7 g/dL, respectively; $p < 0.0001$ for all). Treatment with *Aegle marmelos* extract (AME250, 250 mg/kg p.o.) from Weeks 9 to 16 significantly attenuated liver injury, producing marked reductions in ALT (~107 IU/L, $p < 0.0001$), AST (~163 IU/L, $p < 0.0001$), and ALP (~235 IU/L, $p < 0.0001$), while significantly restoring plasma total protein levels (~6.2 g/dL, $p < 0.01$) relative to the HFD control group. Pioglitazone intervention (PIO20, 20 mg/kg p.o.) fully restored all parameters (ALT ~42 IU/L, AST ~80 IU/L, ALP ~123 IU/L, Total Protein ~6.8 g/dL) to values statistically indistinguishable from the normal diet control group (ND vs PIO20: ns, $p > 0.05$). Consequently, PIO20 demonstrated significantly greater hepatoprotective efficacy compared to AME250 across all four markers ($p < 0.0001$).

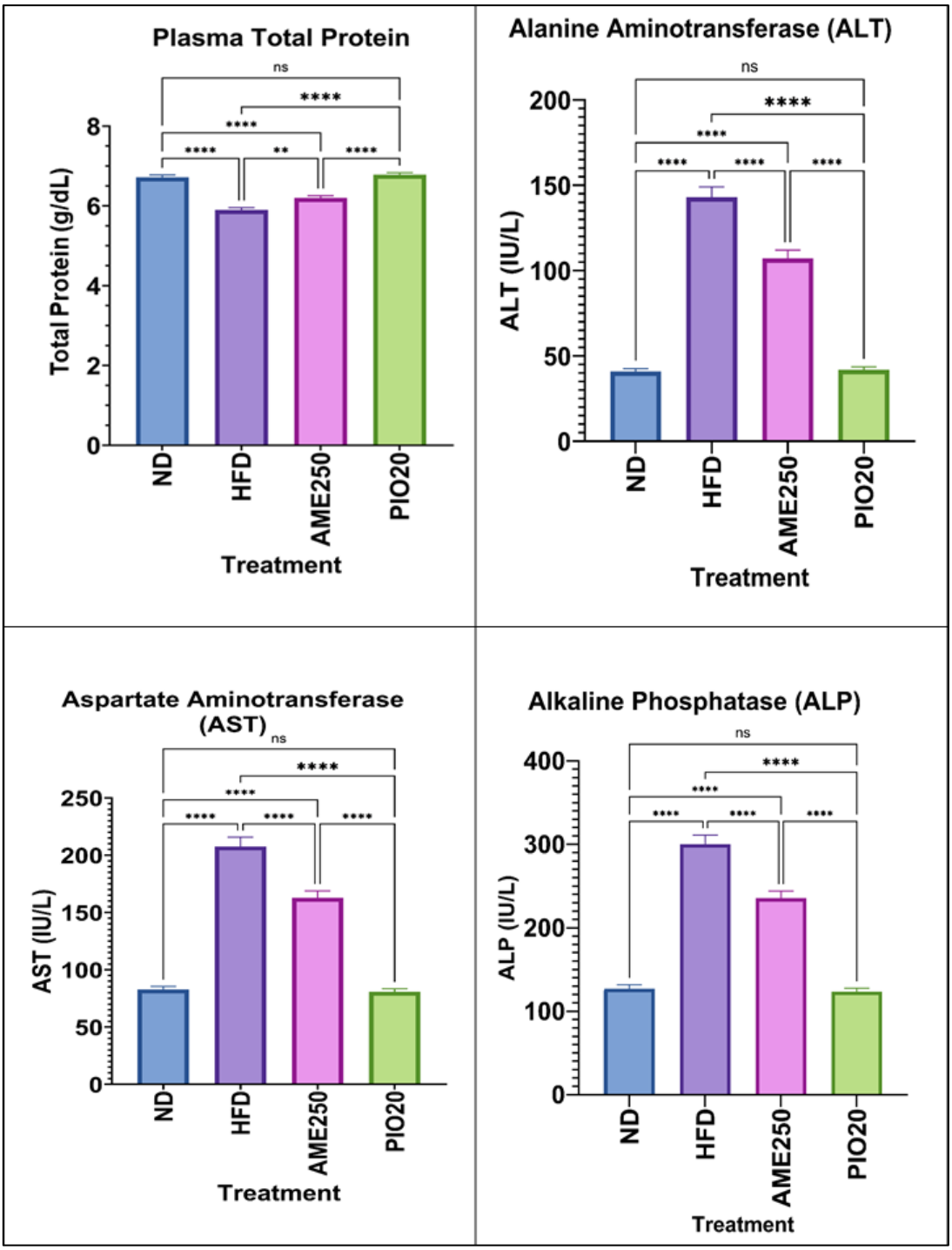

Figure 10. Effects of *Aegle marmelos* extract on plasma total protein, alanine aminotransferase (ALT), aspartate aminotransferase (AST), and alkaline phosphatase (ALP) levels in HFD- and fructose-induced NAFLD in Wistar rat at week 16. Quantifications of (A) Plasma Total Protein (g/dL), (B) Alanine Aminotransferase (ALT, IU/L), (C) Aspartate Aminotransferase (AST, IU/L), and (D) Alkaline Phosphatase (ALP, IU/L) across experimental groups: Normal Diet control (ND), High-Fat Diet + 10% Fructose disease control (HFD), *Aegle marmelos* extract (AME250, 250 mg/kg p.o.), and Pioglitazone (PIO20, 20 mg/kg p.o.). Treatments were administered daily from Week 9 to Week 16. Values represent Mean ± SEM. Statistical significance was determined using ordinary one-way ANOVA followed by Tukey's post-hoc test. **p < 0.01,** ** p < 0.0001, ns = non-significant (p > 0.05).

Natural Resources for Human Health
eISSN: 2583-1194

Effect of *Aegle marmelos* extract on Lipid Profile on animals fed on HFD and fructose

To evaluate the hypolipidemic potential of *Aegle marmelos* extract against diet-induced dyslipidemia, circulating plasma levels of triglycerides, total cholesterol, HDL-C, and LDL-C were measured at Week 16. Sustained administration of a high-fat diet combined with 10% fructose water produced severe atherogenic dyslipidemia, characterized by prominent elevations in triglycerides (~198 mg/dL), total cholesterol (~190 mg/dL), and LDL-C (~128 mg/dL), alongside a marked depletion of protective HDL-C (~23 mg/dL) relative to normal diet controls (~78 mg/dL, ~81 mg/dL, ~21 mg/dL, and ~44 mg/dL, respectively; $p < 0.0001$ for all). Daily oral treatment with *Aegle marmelos* extract (AME250, 250 mg/kg p.o.) from Weeks 9 to 16 significantly attenuated this dyslipidemic profile, decreasing triglycerides (~150 mg/dL, $p < 0.0001$), total cholesterol (~148 mg/dL, $p < 0.0001$), and LDL-C (~85 mg/dL, $p < 0.001$), while producing a significant elevation in HDL-C (~32 mg/dL, $p < 0.01$) compared to the HFD control group. Pioglitazone intervention (PIO20, 20 mg/kg p.o.) exhibited superior lipid-lowering efficacy, fully restoring total cholesterol, HDL-C, and LDL-C concentrations to levels statistically indistinguishable from normal diet controls (ns, $p > 0.05$). Comparative analysis confirmed that PIO20 achieved significantly greater lipid restoration than AME250 across all evaluated parameters ($p < 0.001$ to $p < 0.0001$).

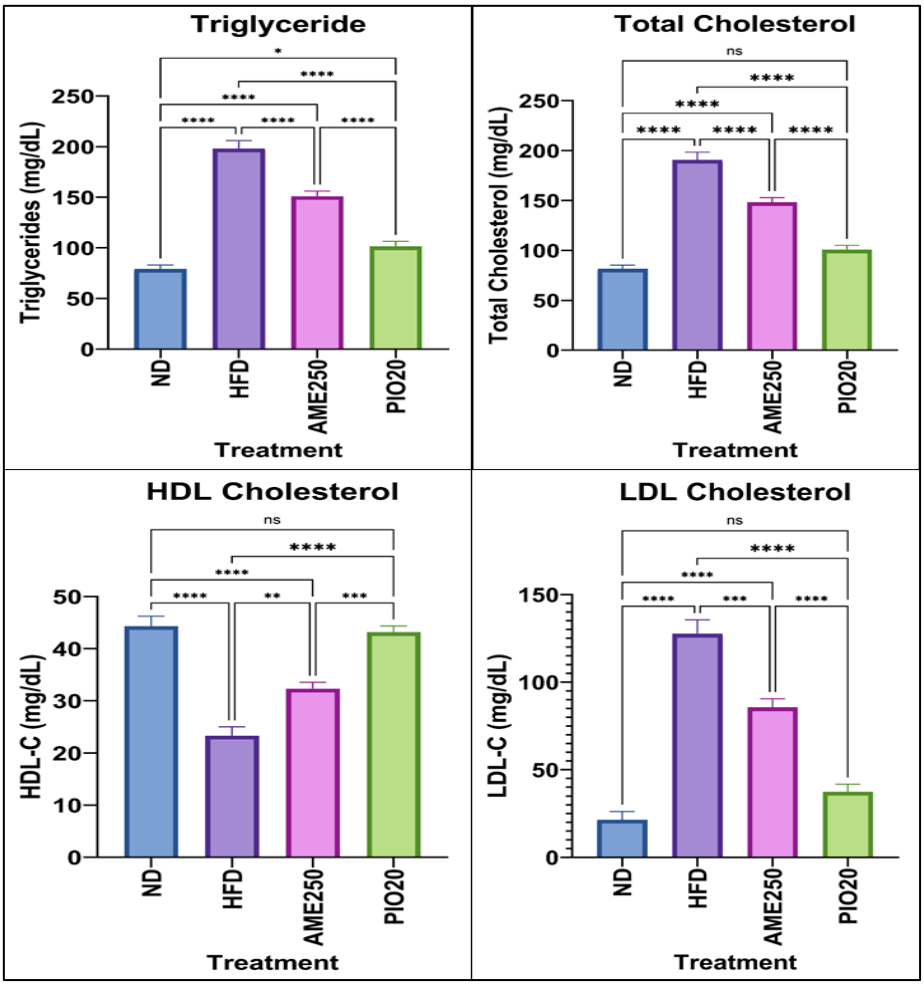

Figure 11. Effect of *Aegle marmelos* extract on plasma triglycerides, total cholesterol, HDL cholesterol, and LDL cholesterol in HFD- and fructose-induced NAFLD in Wistar rats at week 16. Quantifications of (A) Triglyceride (mg/dL), (B) Total Cholesterol (mg/dL), (C) HDL Cholesterol (mg/dL), and (D) LDL Cholesterol (mg/dL) across experimental groups: Normal Diet control (ND), High-Fat Diet + 10% Fructose disease control (HFD), *Aegle marmelos* extract (AME250, 250 mg/kg p.o.), and Pioglitazone (PIO20, 20 mg/kg p.o.). Treatments were administered daily from Week 9 to Week 16. Bars represent Mean ± SEM. Statistical analysis was performed using ordinary one-way ANOVA followed by Tukey's post-hoc test. *$p < 0.05$,* *p < 0.01, *** p < 0.001, **** p < 0.0001, ns = non-significant (p > 0.05).

Natural Resources for Human Health
eISSN: 2583-1194

Effect of *Aegle marmelos* extract on Hepatic Pro-Inflammatory Cytokines on animals fed on HFD and fructose

To evaluate the anti-inflammatory efficacy of *Aegle marmelos* extract in high-fat diet (HFD) and fructose-induced non-alcoholic fatty liver disease (NAFLD), hepatic tissue concentrations of pro-inflammatory cytokines—tumor necrosis factor-alpha (TNF-α), interleukin-1β (IL-1β), and interleukin-6 (IL-6)—were quantified at Week 16. Chronic administration of HFD and fructose induced severe hepatic inflammation, as evidenced by a marked elevation in TNF-alpha (~565 pg/mL), IL-1beta (~430 pg/mL), and IL-6 (~665 pg/mL) levels in the untreated HFD disease-control group compared to normal chow-fed rats (ND: ~140, ~115, and ~190 pg/mL, respectively; $P < 0.0001$ for all).

Treatment with *Aegle marmelos* extract (AME250, 250 mg/kg p.o.) from Week 9 to 16 significantly attenuated the expression of all three hepatic cytokines compared to the HFD group (TNF-α ~305 pg/mL, IL-1β~240 pg/mL, IL-6 ~390 pg/mL; $P < 0.0001$\$). Similarly, administration of the reference standard pioglitazone (PIO20, 20 mg/kg p.o.) robustly suppressed hepatic inflammation, restoring TNF-α, IL-1β, and IL-6 levels back to near-baseline baseline values ($P < 0.0001$ vs. HFD; $P > 0.05$ vs. ND). Although AME250 demonstrated substantial anti-inflammatory capacity, pioglitazone exhibited significantly higher potency in normalizing hepatic cytokine levels across all parameters ($P < 0.0001$\$ vs. AME250).

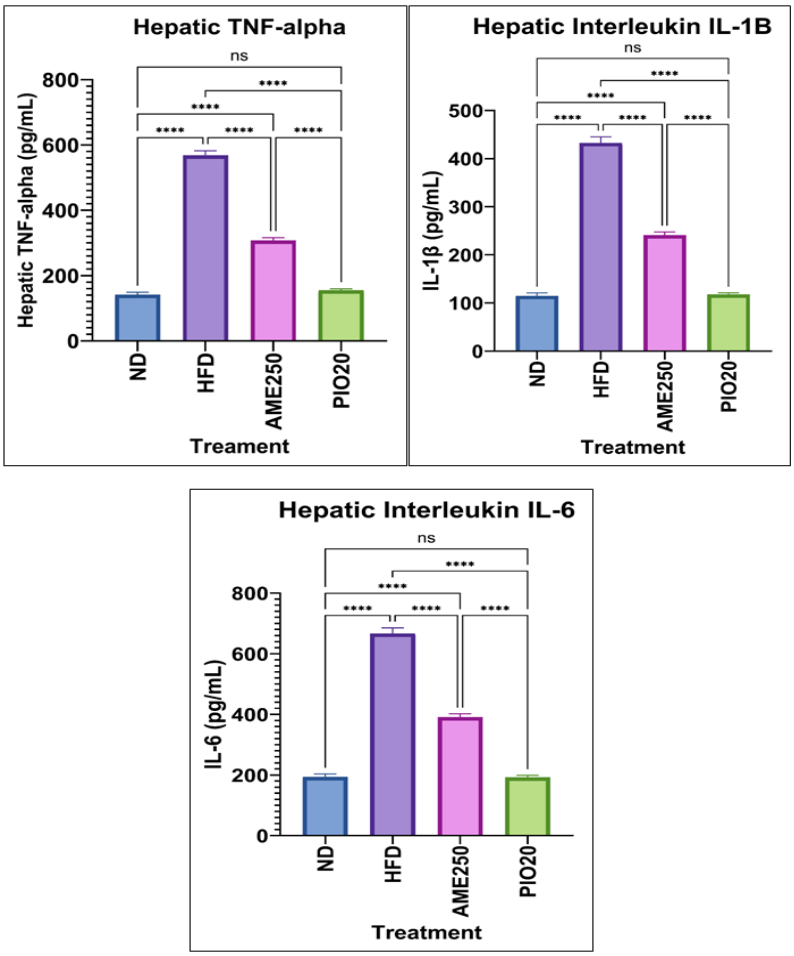

Figure 12. Effect of *Aegle marmelos* extract on hepatic tumor necrosis factor-α (TNF-α), interleukin-1β (IL-1β), and interleukin-6 (IL-6) levels in HFD- and fructose-induced NAFLD in Wistar rats at week 16. Hepatic tissue concentrations of (A) Tumor Necrosis Factor-alpha (TNF-α, pg/mL), (B) Interleukin-1 beta (IL-1β, pg/mL), and (**C**) Interleukin-6 (IL-6, pg/mL) across experimental groups: Normal Diet control (ND), High-Fat Diet + 10% Fructose disease control (HFD), *Aegle marmelos* extract (AME250, 250 mg/kg p.o.), and Pioglitazone (PIO20, 20 mg/kg p.o.). Treatments were administered daily from Week 9 to Week 16. Bars represent Mean ± SEM. Statistical analysis was performed using ordinary one-way ANOVA followed by Tukey's post-hoc test. **** $p < 0.0001$, ns = non-significant ($p > 0.05$).

Effect of *Aegle marmelos* extract on Hepatic Antioxidants on animals fed on HFD and fructose

To determine the antioxidant and anti-peroxidative efficacy of *Aegle marmelos* extract against HFD- and fructose-induced oxidative stress, hepatic catalase, superoxide dismutase (SOD), reduced glutathione (GSH), and malondialdehyde (MDA) levels were evaluated at Week 16. The untreated HFD disease-control group exhibited severe hepatic oxidative stress, characterized by profound depletion of endogenous antioxidant defenses—catalase (~23.5 µmol/mg), SOD (~6.7 µmol/mg) and GSH (~3.0 µmol/mg)—alongside a marked rise in lipid peroxidation product MDA (~4.6 nmol/mg) compared to normal diet controls (~55.5 µmol/mg, ~15.0 µmol/mg, ~7.8 µmol/mg, and ~1.1 nmol/mg, respectively; $p < 0.0001$ for all). Daily oral administration of *Aegle marmelos* extract (AME250, 250 mg/kg p.o.) from Weeks 9 to 16 significantly attenuated oxidative damage, restoring catalase (~33.2 µmol/mg, $p < 0.01$), SOD (~9.8 µmol/mg, $p < 0.01$), and GSH (~4.8 µmol/mg, $p < 0.001$) activities, while significantly suppressing hepatic MDA levels (~3.0 nmol/mg, $p < 0.0001$) relative to the untreated HFD group. Pioglitazone intervention (PIO20, 20 mg/kg p.o.) completely normalized all oxidative markers (catalase ~50.8 µmol/mg, SOD ~14.3 µmol/mg, GSH ~7.4 µmol/mg, MDA ~1.2 nmol/mg) back to levels statistically comparable to normal diet controls (ns, $p > 0.05$). Consequently, PIO20 displayed significantly greater antioxidant restoration and lipid peroxidation suppression than AME250 across all four markers ($p < 0.0001$).

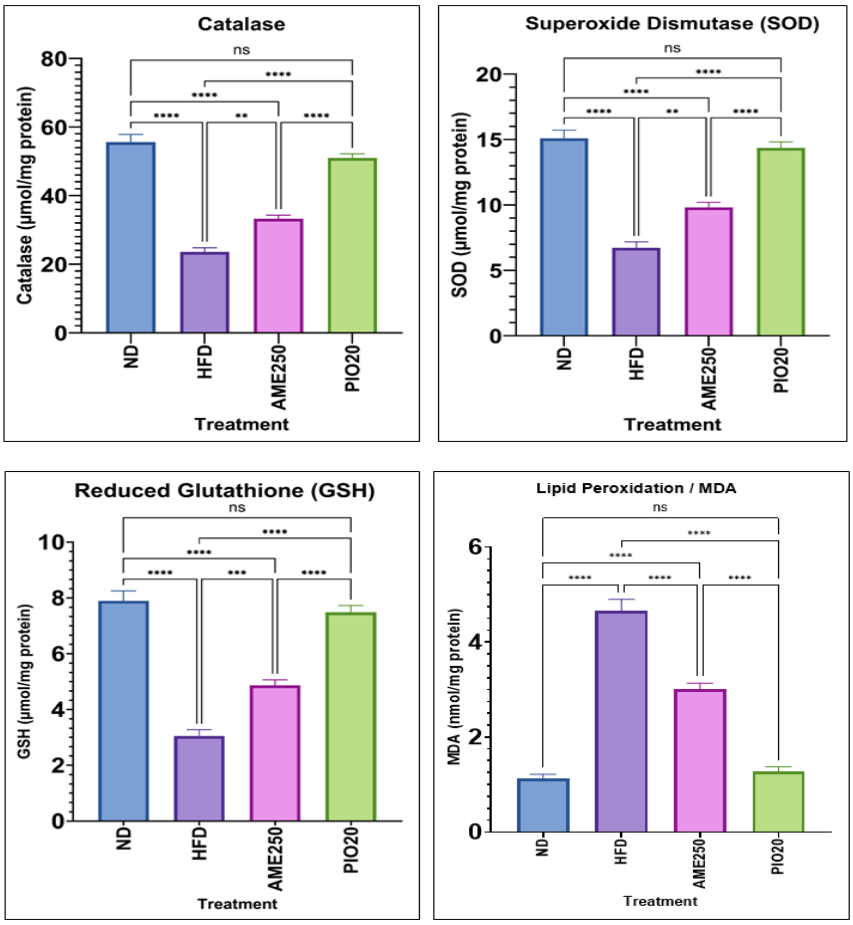

Figure 13. Effect of *Aegle marmelos* extract on hepatic catalase, superoxide dismutase, reduced glutathione (GSH), and lipid peroxidation in HFD- and fructose-induced NAFLD in Wistar rats at week 16. Hepatic tissue levels of (**A**) Catalase (µmol/mg protein), (**B**) Superoxide Dismutase (SOD, µmol/mg protein), (**C**) Reduced Glutathione (GSH, µmol/mg protein), and (**D**) Lipid Peroxidation / Malondialdehyde (MDA, nmol/mg protein) across experimental groups: Normal Diet control (ND), High-Fat Diet + 10% Fructose disease control (HFD), *Aegle marmelos* extract (AME250, 250 mg/kg p.o.), and Pioglitazone (PIO20, 20 mg/kg p.o.). Treatments were administered daily from Week 9 to Week 16. Bars represent Mean ± SEM. Statistical analysis was performed using ordinary one-way ANOVA followed by Tukey's post-hoc test. **$p < 0.01$,** * $p < 0.001$, **** $p < 0.0001$, ns = non-significant ($p > 0.05$).

Effect of *Aegle marmelos* extract on Hepatic Triglyceride Content on animals fed on HFD and fructose

To evaluate the effect of *Aegle marmelos* extract on hepatic lipid accumulation, intrahepatic triglyceride (TG) content was quantified in wet liver tissue at Week 16. Chronic administration of a high-fat diet combined with 10% fructose water induced marked parenchymal steatosis, resulting in a prominent, statistically significant elevation in hepatic TG levels in the untreated HFD group (~48 mg/g wet tissue) compared to normal diet controls (~12 mg/g wet tissue; $p < 0.0001$). Daily intervention with *Aegle marmelos* extract (AME250, 250 mg/kg p.o.) from Weeks 9 to 16 significantly attenuated intrahepatic lipid buildup, reducing hepatic TG levels to ~34 mg/g wet tissue relative to the HFD control group ($p < 0.0001$). Standard treatment with pioglitazone (PIO20, 20 mg/kg p.o.) produced a further reduction in intrahepatic lipid accumulation (~17 mg/g wet tissue, $p < 0.0001$ vs. HFD), though both treatment groups retained slightly higher TG concentrations relative to ND controls ($p < 0.0001$). Comparative evaluation confirmed that pioglitazone achieved significantly greater clearance of hepatic triglycerides than AME250 ($p < 0.0001$).

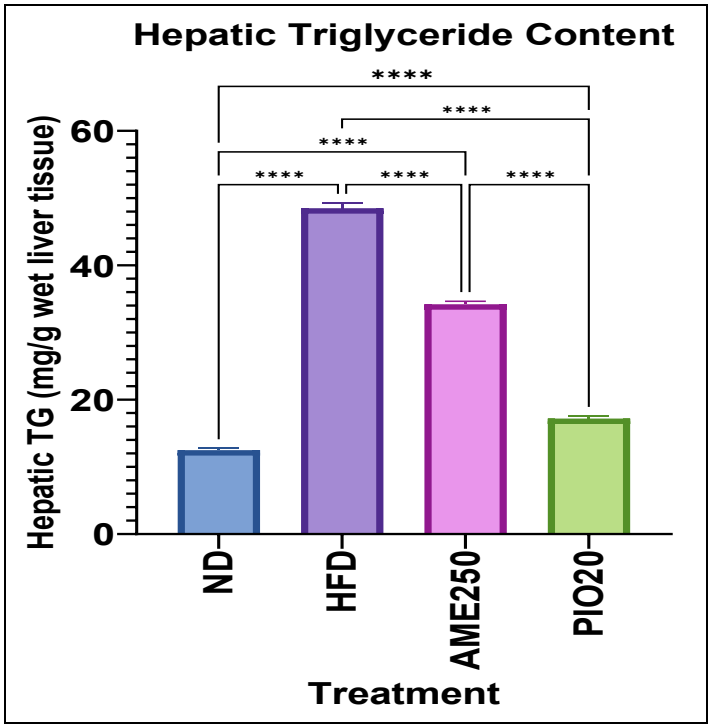

Figure 14. Effect of *Aegle marmelos* extract on hepatic triglyceride content in HFD- and fructose-induced NAFLD in Wistar rats at week 16. Quantification of hepatic triglyceride (TG) content (mg/g wet liver tissue) across experimental groups: Normal Diet control (ND), High-Fat Diet + 10% Fructose disease control (HFD), *Aegle marmelos* extract (AME250, 250 mg/kg p.o.), and Pioglitazone (PIO20, 20 mg/kg p.o.). Treatments were administered daily from Week 9 to Week 16. Values represent Mean ± SEM. Statistical analysis was performed using ordinary one-way ANOVA followed by Tukey's post-hoc test. **** $p < 0.0001$.

Effect of *Aegle marmelos* extract on Gross Morphology and Histopathology of liver tissue

To evaluate the structural hepatoprotective efficacy of *Aegle marmelos* extract, gross morphological inspection and histopathological evaluation of liver tissues were performed at Week 16. Livers harvested from normal diet controls (ND) maintained normal anatomical architecture, deep reddish-brown color, sharp edges, and no detectable histopathological abnormalities (NAD). In contrast, chronic high-fat diet and 10% fructose intake (HFD disease control) induced pronounced gross hepatic pathology, characterized by severe hepatomegaly, rounded organ margins, and diffuse yellowish-pale discoloration reflecting extensive lipid deposition. Histopathological scoring confirmed hepatocellular vacuolar degeneration with inflammatory cell infiltration (Grade <2). Daily treatment with *Aegle marmelos* extract (AME250, 250 mg/kg p.o.) or pioglitazone (PIO20, 20 mg/kg p.o.) from Weeks 9 to 16 completely ameliorated these gross pathological changes, restoring normal organ

dimensions, sharp hepatic margins, and healthy tissue pigmentation, with histopathological assessments revealing no abnormality detected (NAD) across both treatment cohorts.

Figure 15. Gross morphology of liver tissues in HFD- and fructose-induced NAFLD in Wistar rats at week 16. Representative gross anatomical photographs of harvested livers across experimental groups: (**A**) Normal Control (ND), displaying normal reddish-brown color and sharp anatomical margins; (**B**) Disease Control (HFD), displaying severe yellowish-pale discoloration, organ enlargement, and blunted borders indicative of steatosis and cellular swelling; (**C**) *Aegle marmelos* extract (AME250, 250 mg/kg p.o.), showing restoration of normal gross hepatic morphology and color; and (**D**) Pioglitazone (PIO20, 20 mg/kg p.o.), showing complete preservation of healthy liver architecture.

Table 3. Histopathological observations of liver tissue in experimental groups

Experimental Group (n=6)	Histopathological Observation	Histopathological Score/Grade
Normal Control (ND)	No abnormality detected (NAD)	NAD
Disease Control (HFD)	Hepatocellular vacuolar degeneration with infiltration of inflammatory cells	<2
***Aegle marmelos* Extract (AME250)**	No abnormality detected (NAD)	NAD
Pioglitazone (PIO20)	No abnormality detected (NAD)	NAD

Figure Note: ND, normal diet; HFD, high-fat diet; AME250, *Aegle marmelos* extract at 250 mg/kg; PIO20, pioglitazone at 20 mg/kg; NAD, no abnormality detected; WNL, within normal limits. Histopathological changes were graded as follows: NAD/WNL, no abnormality detected/within normal limits; 1, minimal (0–10%); 2, mild (11–20%); 3, moderate (21–40%); and 4, severe (41–100%).

Natural Resources for Human Health
eISSN: 2583-1194

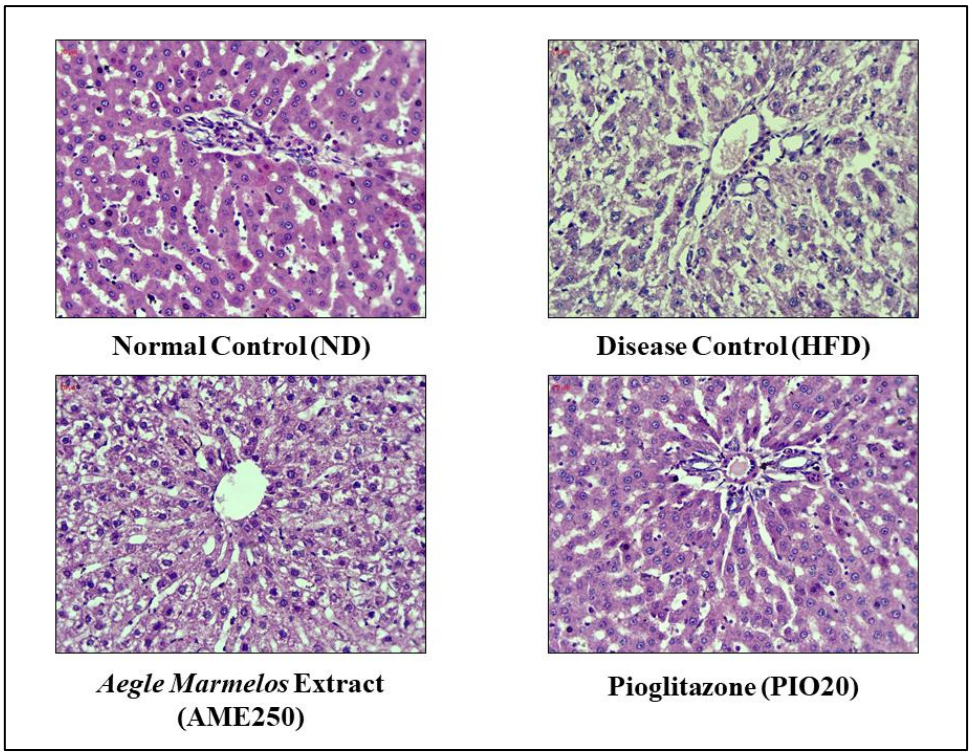

Figure 16. Histopathological evaluation of liver tissues in experimental groups at week 16. Histopathological grading confirmed no abnormality detected (NAD) in ND, AME250, and PIO20 groups, compared to hepatocellular vacuolar degeneration with inflammatory cell infiltration (Grade <2) in the HFD group (n = 6 per group).

4. DISCUSSION

The present study demonstrates that 16 weeks of feeding a high-fat diet (60% energy from fat) together with 10% w/v fructose in drinking water produced a robust experimental phenotype of NAFLD in Wistar rats, recapitulating the principal metabolic and hepatic features of the human disease. Untreated HFD controls developed marked obesity (body weight 420.0 g vs. 250.0 g in normal controls at week 16), elevated BMI, fasting hyperglycemia (187.5 ± 3.81 mg/dL vs. 97.5 ± 3.81 mg/dL), hyperinsulinemia (~46 µIU/mL) with severe insulin resistance (HOMA-IR ~21.3), atherogenic dyslipidemia (triglycerides ~198 mg/dL, total cholesterol ~190 mg/dL, LDL-C ~128 mg/dL with HDL-C suppressed to ~23 mg/dL), hepatomegaly (absolute liver weight ~20.7 g; hepatosomatic index ~4.9%), substantial transaminitis (ALT ~143 IU/L, AST ~208 IU/L, ALP ~300 IU/L), marked intrahepatic triglyceride accumulation (~48 mg/g vs. ~12 mg/g wet tissue), profound depletion of hepatic antioxidant defenses (catalase ~23.5 µmol/mg, SOD ~6.7 µmol/mg, GSH ~3.0 µmol/mg), elevated lipid peroxidation (MDA ~4.6 nmol/mg), increased hepatic pro-inflammatory cytokines, and hepatocellular vacuolar degeneration with inflammatory cell infiltration on histopathology. This simultaneous perturbation of metabolic, oxidative, inflammatory, and structural hepatic parameters closely mirrors the phenotype of human NAFLD; indeed, systematic comparisons of experimental models have identified prolonged high-fat combined with high-fructose feeding as the dietary regimen whose histological and transcriptomic features most closely resemble human NAFLD [48]. The fidelity of the model therefore provides a valid platform for evaluating the antisteatotic and hepatoprotective potential of the A. marmelos extract.

Daily oral administration of the standardized ethanolic extract (AME250, 250 mg/kg) from weeks 9–16 significantly attenuated the HFD/fructose-induced abnormalities across every axis examined. Body weight gain was curtailed (360.0 g vs. 420.0 g) and BMI was reduced (0.7545 ± 0.0088 vs. 0.8698 ± 0.0120) despite food intake remaining unchanged relative to the HFD control group, indicating that the treatment effect was not attributable to reduced caloric consumption but to metabolically mediated improvements in energy homeostasis. Fasting glucose fell to 162.5 ± 3.81 mg/dL, fasting insulin to ~33 µIU/mL, and HOMA-IR to ~13.1, confirming partial restoration of systemic insulin sensitivity. These results are consistent with earlier findings that A. marmelos extracts attenuate fructose-induced hepatic insulin resistance by restoring downstream signaling via Akt and FoxO-1 [34]. Because SREBP-1c is an important transcriptional regulator of hepatic de novo lipogenesis, its involvement provides a

plausible mechanistic link between the improved glycemic and insulinemic status and the concurrent reduction in intrahepatic triglyceride accumulation observed in the AME250 group (~34 mg/g vs. ~48 mg/g) [34].

The extract additionally exerted a clear hypolipidemic action, lowering plasma triglycerides (~150 mg/dL), total cholesterol (~148 mg/dL), and LDL-C (~85 mg/dL), while elevating the protective HDL-C fraction (~32 mg/dL), and simultaneously reducing hepatic triglyceride content. This pattern is consistent with the marmelosin-mediated improvement of glycemia, insulin resistance, lipid profile, and antioxidant status, together with suppression of TNF-α, IL-1β, and IL-6, reported in high-fat diet- and streptozotocin-induced diabetic rats [36], and supports the view that the coumarin constituents of the fruit contribute to its antidyslipidemic activity. The combined reduction in circulating and intrahepatic lipids, without any change in food intake, suggests that the extract modulates hepatic lipid metabolism rather than dietary behavior, an interpretation consistent with inhibition of SREBP-1c-dependent lipogenesis discussed above.

Oxidative stress is a central pathogenic driver in the progression from steatosis to steatohepatitis, and its attenuation is considered a key axis of potential therapeutic intervention. In the present study, AME250 significantly restored hepatic catalytic and non-enzymatic antioxidant capacity—catalase (~33.2 µmol/mg), SOD (~9.8 µmol/mg), and GSH (~4.8 µmol/mg)—while suppressing lipid peroxidation to an MDA level of ~3.0 nmol/mg. These antioxidant effects can be rationally linked to the phytochemical composition of the extract: reversed-phase HPLC standardization identified umbelliferone (39.38 ppm) as the predominant marker, followed by quercetin (19.48 ppm) and aegeline (18.32 ppm). Quercetin is a well-established flavonoid radical scavenger [65], and polyphenol-rich A. marmelos preparations have previously been shown to ameliorate serum glucose, dyslipidemia, pro-inflammatory cytokine levels (TNF-α, IL-6, IL-1β), and antioxidant status in diabetic mice, with cytoprotective activity against hyperglycemia-induced oxidative stress in HepG2 cells [40]. The observed suppression of hepatic TNF-α, IL-1β, and IL-6 in the AME250 group—alongside the complete return of liver histology to "no abnormality detected" status, in contrast to the vacuolar degeneration and inflammatory infiltration of the untreated HFD group—indicates that the extract's antioxidant capacity translates into reduced inflammatory signaling and structural hepatoprotection. The near-complete histological recovery is particularly notable given that hepatic triglyceride levels, although substantially reduced, remained above the normal-control range, suggesting that the extract may exert cytoprotective and anti-inflammatory effects that extend beyond simple lipid clearance.

The positive control, pioglitazone (20 mg/kg), produced greater improvements than AME250 across most endpoints, fully normalizing liver enzymes, lipid profile, antioxidant status, and hepatosomatic index to values statistically indistinguishable from normal controls. This superiority is expected, since pioglitazone, a PPARγ agonist, is a guideline-supported pharmacotherapy that can be considered in patients with biopsy-proven NASH with or without type 2 diabetes [16]; the comparison confirms the internal validity of the model and provides a clinically relevant benchmark for the plant extract. Nevertheless, the broad-spectrum activity of AME250—simultaneously improving adiposity, glycemia, insulin resistance, dyslipidemia, hepatic steatosis, oxidative stress, inflammation, and histopathology—suggests that the bioactivity of its marker compounds (umbelliferone, quercetin, and aegeline) may contribute to its metabolic effects [66,67], although equivalence to an established insulin sensitizer remains untested. Several limitations of this study should be acknowledged. The number of animals per group (n = 6) was modest; a single dose of the extract (250 mg/kg) was evaluated without a dose–response design; and hepatic molecular signaling (e.g., AMPK, SREBP-1c, PPAR-α, Nrf2) was not directly assessed, so the proposed mechanisms remain inferential. Future studies incorporating dose-ranging, longer treatment periods, and transcriptomic or protein-level pathway analyses—together with evaluation of the individual marker compounds—would strengthen the mechanistic evidence base. Within these limits, the present data support the standardized ethanolic extract of A. marmelos fruit as a promising adjunctive candidate for the management of NAFLD and its associated metabolic disturbances.

CONCLUSION

In conclusion, the standardized ethanolic extract of *Aegle marmelos* significantly ameliorates high-fat diet and fructose-induced Non-Alcoholic Fatty Liver Disease (NAFLD) in Wistar rats. Oral intervention with the ethanolic extract improves systemic insulin sensitivity, lowers intrahepatic triglyceride accumulation, mitigates lipid peroxidation, restores endogenous antioxidant capacity, reduces pro-inflammatory cytokine expression, and preserves normal hepatic histological structure. These therapeutic properties are mediated by the synergistic bioactivity of its key marker compounds—umbelliferone, quercetin, and aegeline—supporting the potential of the ethanolic extract of *Aegle marmelos* as a promising natural candidate for managing NAFLD and associated metabolic disorders.

LIST OF ABBREVIATIONS

- A. marmelos: *Aegle marmelos*
- AMPK: AMP-activated protein kinase
- HFD: High-fat diet
- ND: Normal diet
- NASH: Non-alcoholic steatohepatitis
- MAFLD: Metabolic dysfunction-associated fatty liver disease
- HPLC: High-performance liquid chromatography
- NAFLD: Non-alcoholic fatty liver disease
- NF-ϰB: Nuclear factor-kappa B
- Nrf2: Nuclear factor erythroid 2-related factor 2
- SREBP-1c: Sterol regulatory element-binding protein 1c
- PBS: Phosphate-buffered saline
- MDA: Malondialdehyde
- AMPK: AMP-activated protein kinase
- ACC: Acetyl-CoA carboxylase
- PPAR-α: Peroxisome proliferator-activated receptor alpha
- SOD: Superoxide dismutase
- GSH: Reduced glutathione
- HOMA-IR: Homeostatic Model Assessment of Insulin Resistance
- DTNB: 5,5'-dithiobis-(2-nitrobenzoic acid)
- TBARS: Thiobarbituric Acid Reactive Substances
- NBT: Nitroblue tetrazolium
- Akt: Protein kinase B
- FoxO: Forkhead box protein O

ETHICS APPROVAL AND CONSENT TO PARTICIPATE

All experimental procedures were conducted in accordance with the guidelines of the Committee for the Purpose of Control and Supervision of Experiments on Animals (CPCSEA) [68], Government of India, and were approved by the Institutional Animal Ethics Committee (IAEC) under approval No. IAEC/CPD/415/11. The study was conducted at the Animal House of Smt. Sharadchandrika Suresh Patil College of Pharmacy, Chopda, Jalgaon, Maharashtra, India, registered with CPCSEA under Registration No. 316/PO/ReBi/S/2000/CPCSEA, dated 02/11/2022. All applicable ethical and regulatory requirements for the use and care of experimental animals were duly followed.

HUMAN AND ANIMAL RIGHTS

Research Involving Animals

All *in vivo* experiments were conducted in accordance with the guidelines of the Committee for the Purpose of Control and Supervision of Experiments on Animals (CPCSEA), Government of India, and the Guide for the Care and Use of Laboratory Animals, 8th edition, published by the National Research Council, National Academies. The experimental protocol was

reviewed and approved by the Institutional Animal Ethics Committee (IAEC) under approval No. IAEC/CPD/415/11. The study was conducted at the Animal House of Smt. Sharadchandrika Suresh Patil College of Pharmacy, Chopda, Jalgaon, Maharashtra, India, registered with CPCSEA under Registration No. 316/PO/ReBi/S/2000/CPCSEA, dated 02/11/2022.

Research Involving Plants

The plant material used in the present study, *Aegle marmelos*, was collected from local areas of Nashik, Maharashtra, India, during the winter season. Healthy, ripe fruits were collected in accordance with applicable local and national regulations. The plant material was authenticated by the Western Regional Centre, Botanical Survey of India (BSI), Pune, and a voucher specimen (BSI/WRC/Tech./2025/PSB-110, Specimen No. 02) was deposited in the herbarium of the Western Regional Centre, Botanical Survey of India, Pune. The study used *Aegle marmelos*, which is classified as Near Threatened [69], and the collection and use of the plant material complied with relevant guidelines for plant research and applicable conservation regulations, including those concerning species protected under IUCN and CITES provisions.

CONFLICT OF INTEREST

The authors declare that there are no conflicts of interest regarding the publication of this research.

ACKNOWLEDGEMENT

The author gratefully acknowledges Smt. Sharadchandrika Suresh Patil College of Pharmacy, Chopda, Jalgaon, Maharashtra, India, for providing the necessary facilities and support to carry out this research work. The author also sincerely thanks RAP Analytical Research Private Limited, Nashik, for HPLC analysis and Biotox Laboratories, Nashik, for biochemical parameter estimation and their valuable technical assistance.

REFERENCES

[1] Godoy-Matos AF, Júnior WSS, Valério CM. NAFLD as a continuum: from obesity to metabolic syndrome and diabetes. Diabetology & Metabolic Syndrome [Internet]. 2020 July 14 [cited 2026 Jan];12(1):60. Available from: https://doi.org/10.1186/s13098-020-00570-y

[2] Berardo C, Pasqua LGD, Cagna M, Richelmi P, Vairetti M, Ferrigno A. Nonalcoholic Fatty Liver Disease and Non-Alcoholic Steatohepatitis: Current Issues and Future Perspectives in Preclinical and Clinical Research. International Journal of Molecular Sciences [Internet]. 2020 Dec 17 [cited 2025 Nov];21(24):9646. Available from: https://doi.org/10.3390/ijms21249646

[3] Deore AB, Mohammed Rageeb MU. Pathogenesis of Non-Alcoholic Fatty Liver Disease and Non-Alcoholic Steatohepatitis. YMER Journal [Internet]. 2023 Jan 1 [cited 2025 Nov];22(12):94–105. Available from: https://doi.org/10.13140/rg.2.2.25224.80643

[4] Qureshi K. Metabolic liver disease of obesity and role of adipose tissue in the pathogenesis of nonalcoholic fatty liver disease. World Journal of Gastroenterology [Internet]. 2007 Jan 1 [cited 2026 Jan];13(26):3540. Available from: https://doi.org/10.3748/wjg.v13.i26.3540

[5] Teng ML, Ng CH, Huang DQ, Chan KE, Tan DJ, Lim WH, et al. Global incidence and prevalence of nonalcoholic fatty liver disease. Clinical and Molecular Hepatology [Internet]. 2022 Dec 15 [cited 2026 Jan];29. Available from: https://doi.org/10.3350/cmh.2022.0365

[6] Rinella ME, Lazarus JV, Ratziu V, Francque S, Sanyal AJ, Kanwal F, et al. A multisociety Delphi consensus statement on new fatty liver disease nomenclature. Journal of Hepatology [Internet]. 2023 June 24 [cited 2026 Mar];79(6):1542–56. Available from: https://doi.org/10.1016/j.jhep.2023.06.003

[7] Sohn W, Lee Y, Kim SS, Kim JH, Jin Y, Kim GA, et al. KASL clinical practice guidelines for the management of metabolic dysfunction-associated steatotic liver disease 2025. Clinical and Molecular Hepatology [Internet]. 2025 Feb 19 [cited 2026 Mar];31. Available from: https://doi.org/10.3350/cmh.2025.0045

[8] Buzzetti E, Pinzani M, Tsochatzis EA. The multiple-hit pathogenesis of non-alcoholic fatty liver disease (NAFLD). Metabolism. 2016;

[9] Wang B, Yang R, Zhu Y, Xing J, Lou X, He Y, et al. Involvement of xanthine oxidase and paraoxonase 1 in the process of oxidative stress in nonalcoholic fatty liver disease. Molecular Medicine Reports [Internet]. 2016 Dec 12 [cited 2026 Jan];15(1):387–95. Available from: https://doi.org/10.3892/mmr.2016.6025

[10] Wong SK, Chin K, Ahmad F, Soelaiman IN. Biochemical and histopathological assessment of liver in a rat model of metabolic syndrome induced by high-carbohydrate high-fat diet. Journal of Food Biochemistry [Internet]. 2020 Aug 3 [cited 2026 Mar];44(10). Available from: https://doi.org/10.1111/jfbc.13371

[11] Carmiel-Haggai M, Cederbaum AI, Nieto N. A high-fat diet leads to the progression of non-alcoholic fatty liver disease in obese rats. The FASEB Journal [Internet]. 2004 Nov 2 [cited 2025 Nov];19(1):136–8. Available from: https://doi.org/10.1096/fj.04-2291fje

[12] Peng C, Stewart AG, Woodman OL, Ritchie RH, Qin CX. Non-Alcoholic Steatohepatitis: A Review of Its Mechanism, Models and Medical Treatments. Frontiers in Pharmacology [Internet]. 2020 Dec 3 [cited 2026 Jan];11:603926. Available from: https://doi.org/10.3389/fphar.2020.603926

[13] Free fatty acids, not triglycerides, are associated with non-alcoholic liver injury progression in high fat diet induced obese rats [Internet]. [cited 2026 Jan]. Available from: https://doi.org/10.1186/s12944-016-0194-7

[14] Polyzos SA, Kechagias S, Tsochatzis E. Review article: non-alcoholic fatty liver disease and cardiovascular diseases: associations and treatment considerations. Alimentary Pharmacology & Therapeutics [Internet]. 2021 Aug 20 [cited 2025 Nov];54(8):1013–25. Available from: https://doi.org/10.1111/apt.16575

[15] Malespin M, Barritt AS, Watkins S, Schoen C, Tincopa MA, Corbin KD, et al. Weight Loss and Weight Regain in Usual Clinical Practice: Results From the TARGET-NASH Observational Cohort. Clinical Gastroenterology and Hepatology [Internet]. 2021 Jan 21 [cited 2026 Jan];20(10):2393. Available from: https://doi.org/10.1016/j.cgh.2021.01.023

[16] Negi CK, Babica P, Bajard L, Bienertova-vasku J, Tarantino G. Insights into the molecular targets and emerging pharmacotherapeutic interventions for nonalcoholic fatty liver disease. Metabolism. 2022;

[17] Bhar K, Mondal S, Suresh P. An Eye-Catching Review of Aegle marmelos L. (Golden Apple). Pharmacognosy Journal [Internet]. 2019 Feb 18 [cited 2026 Mar];11(2):207–24. Available from: https://doi.org/10.5530/pj.2019.11.34

[18] Dhankhar eep, Ruhil S, Balhara M, Dhankhar S, Chhillar AK. Aegle marmelos (Linn.) Correa: A potential source of Phytomedicine. Journal of Medicinal Plants Research [Internet]. 2011 May 4 [cited 2025 Oct];5(9):1497–507. Available from: https://africaneditors.org/journal/JMPR/full-text-pdf/91551-128840

[19] Sharma N, Radha, Kumar M, Zhang B, Kumari N, Singh D, et al. Aegle marmelos (L.) Correa: An Underutilized Fruit with High Nutraceutical Values: A Review. International Journal of Molecular Sciences [Internet]. 2022 Sept 17 [cited 2026 May];23(18):10889. Available from: https://doi.org/10.3390/ijms231810889

[20] Narender T, Shweta S, Tiwari P, Reddy KP, Khaliq T, Prathipati P, et al. Antihyperglycemic and antidyslipidemic agent from Aegle marmelos. Bioorganic & Medicinal Chemistry Letters [Internet]. 2006 Dec 16 [cited 2026 Aug];17(6):1808–11. Available from: https://doi.org/10.1016/j.bmcl.2006.12.037

[21] Aggarwal H, Nair J, Sharma P, Sehgal R, Naeem U, Rajora P, et al. Aegle marmelos differentially affects hepatic markers of glycolysis, insulin signalling pathway, hypoxia, and inflammation in HepG2 cells grown in fructose versus glucose-rich environment. Molecular and Cellular Biochemistry. 2018;

[22] Rathee D, Kamboj A, Sachdev RK, Sidhu S. Hepatoprotective effect of Aegle marmelos augmented with piperine co-administration in paracetamol model. Revista Brasileira de Farmacognosia [Internet]. 2017 Dec 15 [cited 2026 May];28(1):65–72. Available from: https://doi.org/10.1016/j.bjp.2017.11.003

[23] Rathee D, Kamboj A, Sidhu S. Augmentation of hepatoprotective potential of Aegle marmelos in combination with piperine in carbon tetrachloride model in wistar rats. Chemistry Central Journal [Internet]. 2018 Aug 20 [cited 2026 Aug];12(1):94. Available from: https://pubmed.ncbi.nlm.nih.gov/30123925/

[24] Benni JM, Jayanthi MK, Suresha RN. Evaluation of the anti-inflammatory activity of Aegle marmelos (Bilwa) root. Indian Journal of Pharmacology. 2011;43(4).

[25] Sabu MC, Kuttan R. ANTIDIABETIC ACTIVITY OF AEGLE MARMELOS AND ITS RELATIONSHIP WITH ITS ANTIOXIDANT PROPERTIES. PubMed. 2004;48(1).

[26] Pynam H, Dharmesh SM. Antioxidant and anti-inflammatory properties of marmelosin from Bael (Aegle marmelos L.); Inhibition of TNF-α mediated inflammatory/tumor markers. Biomedicine and Pharmacotherapy. 2018;

[27] Vijaya C, Ramanathan M, Suresh B. Lipid lowering activity of ethanolic extract of leaves of Aegle marmelos (Linn.) in hyperlipidaemic models of Wistar albino rats. PubMed [Internet]. 2009 Mar 1 [cited 2025 Nov];47(3):182–5. Available from: https://pubmed.ncbi.nlm.nih.gov/19405383

[28] Bhuvaneswari R, Sasikumar K. ANTIHYPERLIPIDEMIC ACTIVITY OF Aegle marmelos (L) Corr., LEAF EXTRACT IN TRITON WR-1339 INDUCED HYPERLIPIDEMIC RATS. 2013.

[29] Devi KP, Sivaraj A, Kumar PV, Ahmed K, Sathiyaraj K, Kumar BSA, et al. Hypolipidemic effect of Aegle marmelos leaf extract in streptozotocin (STZ) induced diabetic male albino rats. International Journal of PharmTech Research [Internet]. 2010 Jan 1 [cited 2025 Oct];2(1):259–65. Available from: http://sphinxsai.com/sphinxsaiVol_2No.1/PharmTech_Vol_2No.1/PharmTech_Vol_2No.1PDF/PT=41%20(259-265).pdf

[30] Kamalakkannan N, Prince PSM. Antihyperlipidaemic effect of Aegle marmelos fruit extract in streptozotocin-induced diabetes in rats. Journal of the Science of Food and Agriculture [Internet]. 2004 Nov 26 [cited 2025 Nov];85(4):569–73. Available from: https://doi.org/10.1002/jsfa.1978

[31] Asghar N, Mushtaq Z, Arshad MU, Imran M, Ahmad RS, Hussain SM. Phytochemical composition, antilipidemic and antihypercholestrolemic perspectives of Bael leaf extracts. Lipids in Health and Disease [Internet]. 2018 Apr 3 [cited 2026 Jan];17(1):68. Available from: https://doi.org/10.1186/s12944-018-0713-9

[32] Ansari P, Afroz N, Jalil S, Azad SB, Mustakim G, Anwar S, et al. (L.) corr. is partly mediated by increased insulin secretion, α-amylase inhibition, and retardation of glucose absorption. Journal of Pediatric Endocrinology and Metabolism. 2016;30(1).

[33] Gandhi GR, Ignacimuthu S, Paulraj MG. Hypoglycemic and β-cells regenerative effects of Aegle marmelos (L.) Corr. bark extract in streptozotocin-induced diabetic rats. Food and Chemical Toxicology. 2012;

[34] Nair J, Velpandian T, Das US, Sharma P, Nag TC, Mathur S, et al. Molecular and Metabolic Markers of Fructose Induced Hepatic Insulin Resistance in Developing and Adult Rats are Distinct and Aegle marmelos is an Effective Modulator. Scientific Reports [Internet]. 2018 Oct 23 [cited 2026 May];8(1):15950. Available from: https://doi.org/10.1038/s41598-018-33503-x

[35] Ibrahim NA, Mohammed MMD, Aly HF, Ali SA, Al-Hady DA. Efficiency of the leaves and fruits of Aegle marmelos methanol extract (L.) Correa and their relative hepatotoxicity induced by CCL4 and identification of their active constituents by using LC/MS/MS. Toxicology Reports [Internet]. 2018 Jan 1 [cited 2026 May];5:1161–8. Available from: https://doi.org/10.1016/j.toxrep.2018.09.005

[36] Alenezi SK, Alharbi SK, Alsahli T, Alqahtani R, Afzal MA, Sharma KK, et al. Marmelosin Protects Against Metabolic Disturbances in High-Fat Diet and Streptozotocin-Induced Diabetes. Diabetes Metabolic Syndrome and Obesity [Internet]. 2025 Dec 1 [cited 2026 May];4769–85. Available from: https://doi.org/10.2147/dmso.s566221

[37] Sharshar AM, Ameen AA, El-Masry H. bioactive role of aqueous extract of aegle marmelos leaves on obese rats. International Journal of Health Sciences [Internet]. 2022 Aug 29 [cited 2025 Nov];620–9. Available from: https://doi.org/10.53730/ijhs.v6ns9.12260

[38] Thirunalasundari PS and T. Hepatoprotective Activity of Aegle marmelos in CCl4 Induced Toxicity - An In-vivo Study. The Journal of Phytology [Internet]. 2011 Aug 17 [cited 2025 Oct];3(9):5–9. Available from: https://scienceflora.org/journals/index.php/jp/article/view/2295

[39] Haas JT, Francque S, Staels B. Pathophysiology and Mechanisms of Nonalcoholic Fatty Liver Disease. Annual Review of Physiology. 2015;78(1).

[40] Ibrahim M, Parveen B, Zahiruddin S, Gautam G, Parveen R, Khan MA, et al. Analysis of polyphenols in Aegle marmelos leaf and ameliorative efficacy against diabetic mice through restoration of antioxidant and anti-inflammatory status. Journal of Food Biochemistry [Internet]. 2021 July 11 [cited 2026 Mar];46(4). Available from: https://doi.org/10.1111/jfbc.13852

[41] Das K, Tiwari RK, Shrivastava DK. Techniques for evaluation of medicinal plant products as antimicrobial agents: Current methods and future trends. Journal of Medicinal Plants Research [Internet]. 2010 Jan 18 [cited 2025 Oct];4(2):104–11. Available from: https://www.academicjournals.org/article/article1380375549_Das%20et%20al.pdf

[42] Venthodika A, Chhikara N, Mann S, Garg MK, Sofi SA, Panghal A. Bioactive compounds of Aegle marmelos L., medicinal values and its food applications: A critical review. Phytotherapy Research. 2021;

[43] Varughese B, Tripathi J. Phytochemical Evaluation of different Solvent Extracts of Aegle marmelos fruit at different Stages of its Ripening. Journals & Books Hosting (International Knowledge Sharing Platform). 2013;8.

[44] Shinde PB, Katekhaye SD, Mulik MB. Rapid simultaneous determination of marmelosin, umbelliferone and scopoletin from Aegle marmelos fruit by RP-HPLC. Journal of Food Science and Technology. 2014;51(9).

[45] Bansal Y, Bansal G. Analytical methods for standardization of Aegle marmelos: A review. JournL of Pharmaceutical Education Research. 2011;

[46] Kučera O, Garnol T, Lotková H, Staňková P, Mazurová Y, Hroch M, et al. The Effect of Rat Strain, Diet Composition and Feeding Period on the Development of a Nutritional Model of Non-Alcoholic Fatty Liver Disease in Rats. Physiological Research [Internet]. 2011 Apr 16 [cited 2025 Nov];60(2):317–28. Available from: https://doi.org/10.33549/physiolres.932022

[47] Crescenzo R, Bianco F, Coppola P, Mazzoli A, Tussellino M, Carotenuto R, et al. Fructose supplementation worsens the deleterious effects of short-term high-fat feeding on hepatic steatosis and lipid metabolism in adult rats. Experimental Physiology [Internet]. 2014 June 28 [cited 2025 Nov];99(9):1203–13. Available from: https://doi.org/10.1113/expphysiol.2014.079632

[48] Im YR, Hunter H, Hahn D de G, Duret A, Cheah Q, Dong J, et al. A Systematic Review of Animal Models of NAFLD Finds High-Fat, High-Fructose Diets Most Closely Resemble Human NAFLD. Hepatology [Internet]. 2021 May 11 [cited 2025 Nov];74(4):1884–901. Available from: https://doi.org/10.1002/hep.31897

[49] Bagnol D, Al-Shamma H, Behan DP, Whelan K, Grottick AJ. Diet-Induced Models of Obesity (DIO) in Rodents. Current Protocols in Neuroscience [Internet]. 2012 Apr 1 [cited 2025 Nov];59(1). Available from: https://doi.org/10.1002/0471142301.ns0938s59

[50] Morrow T. Animal Models of Painful Diabetic Neuropathy: The STZ Rat Model. Deep Blue (University of Michigan) [Internet]. 2004 Oct 1 [cited 2025 Nov];29(1). Available from: https://hdl.handle.net/2027.42/153112

[51] Langnes Ø, Eriksen E, Folkvord A. Liver condition of 0 and 1-group cod (Gadus morhua) in the Barents Sea. Marine Biology [Internet]. 2023 Dec 27 [cited 2025 Dec];171(2). Available from: https://doi.org/10.1007/s00227-023-04354-6

[52] Clouthier DE, Comerford SA, Hammer RE. Hepatic fibrosis, glomerulosclerosis, and a lipodystrophy-like syndrome in PEPCK-TGF-beta1 transgenic mice. Journal of Clinical Investigation [Internet]. 1997 Dec 1 [cited 2026 Jan];100(11):2697–713. Available from: https://doi.org/10.1172/jci119815

[53] Barssotti L, Abreu ICME de, Brandão ABP, Albuquerque RCMF de, Ferreira FG, Salgado MAC, et al. Saccharomyces boulardii modulates oxidative stress and renin angiotensin system attenuating diabetes-induced liver injury in mice. Scientific Reports [Internet]. 2021 Apr 28 [cited 2026 Jan];11(1):9189. Available from: https://doi.org/10.1038/s41598-021-88497-w

[54] Essa HA, El-Metwally AE, Elkady NA. The potential protective effects of fermented extra virgin olive oil on high-fructose diet-induced non-alcoholic steatohepatitis in rats. Food Production Processing and Nutrition [Internet]. 2025 Sept 9 [cited 2026 Mar];7(1). Available from: https://doi.org/10.1186/s43014-025-00320-5

[55] Bhatt MP, Rai N, Pokhrel S, Acharya P, Marhatta SB, Khanal DP, et al. Standardization of Visible Kinetic Assay for the Estimation of Plasma Glucose by Glucose Oxidase and Peroxidase Method. Journal of Manmohan Memorial Institute of Health Sciences [Internet]. 2021 Dec 1 [cited 2026 Feb];7(1):49–59. Available from: https://doi.org/10.3126/jmmihs.v7i1.43150

[56] Matthews DR, Hosker JP, Rudenski A, Naylor BA, Treacher D, Turner RC. Homeostasis model assessment: insulin resistance and ?-cell function from fasting plasma glucose and insulin concentrations in man. Diabetologia [Internet]. 1985 July 1 [cited 2026 Aug];28(7):412–9. Available from: https://doi.org/10.1007/BF00280883

[57] Okita K, Iwahashi H, Kozawa J, Okauchi Y, Funahashi T, Imagawa A, et al. Homeostasis model assessment of insulin resistance for evaluating insulin sensitivity in patients with type 2 diabetes on insulin therapy. Endocrine Journal [Internet]. 2012 Nov 9 [cited 2025 Nov];60(3):283–90. Available from: https://doi.org/10.1507/endocrj.ej12-0320

[58] Aebi H. [13] Catalase in vitro. In: Methods in enzymology on CD-ROM/Methods in enzymology [Internet]. Academic Press; 1984 [cited 2026 Aug]. p. 121–6. Available from: https://doi.org/10.1016/s0076-6879(84)05016-3

[59] Kono Y. Generation of superoxide radical during autoxidation of hydroxylamine and an assay for superoxide dismutase. Archives of Biochemistry and Biophysics [Internet]. 1978 Feb 1 [cited 2026 Aug];186(1):189–95. Available from: https://doi.org/10.1016/0003-9861(78)90479-4

[60] MORON M, DePierre JW, Mannervik B. Levels of glutathione, glutathione reductase and glutathione S-transferase activities in rat lung and liver. Biochimica et Biophysica Acta (BBA) - General Subjects [Internet]. 1979 Jan 4 [cited 2026 Aug];582(1):67–78. Available from: https://doi.org/10.1016/0304-4165(79)90289-7

[61] Ohkawa H, Ohishi N, Yagi K. Assay for lipid peroxides in animal tissues by thiobarbituric acid reaction. Analytical Biochemistry [Internet]. 1979 June 1 [cited 2026 Aug];95(2):351–8. Available from: https://doi.org/10.1016/0003-2697(79)90738-3

[62] Butler WM, Maling HM, Horning MG, BRODIE BB. The direct determination of liver triglycerides. Journal of Lipid Research [Internet]. 1961 Jan 1 [cited 2026 Aug];2(1):95–6. Available from: https://doi.org/10.1016/s0022-2275(20)39047-7

[63] Shackelford C, Long GG, Wolf JC, Okerberg CV, Herbert R. Qualitative and Quantitative Analysis of Nonneoplastic Lesions in Toxicology Studies. Toxicologic Pathology [Internet]. 2002 Jan 1 [cited 2026 Sept];30(1):93–6. Available from: https://doi.org/10.1080/01926230252824761

[64] Mann PC, Vahle JL, Keenan CM, Baker JF, Bradley A, Goodman DG, et al. International Harmonization of Toxicologic Pathology Nomenclature. Toxicologic Pathology [Internet]. 2012 May 25 [cited 2026 Aug];40. Available from: https://doi.org/10.1177/0192623312438738

[65] Sak K. Dependence of DPPH Radical Scavenging Activity of Dietary Flavonoid Quercetin on Reaction Environment. Mini-Reviews in Medicinal Chemistry [Internet]. 2014 June 22 [cited 2026 Jan];14(6):494–504. Available from: https://doi.org/10.2174/1389557514666140622204037

[66] Tiwari R, Mishra S, Danaboina G, Jadaun GPS, Kalaivani M, Kalaiselvan V, et al. Comprehensive chemo-profiling of coumarins enriched extract derived from Aegle marmelos (L.) Correa fruit pulp, as an anti-diabetic and anti-inflammatory agent. PubMed Central [Internet]. 2023 July 25 [cited 2026 Jan];31(9):101708. Available from: https://www.ncbi.nlm.nih.gov/pmc/articles/10410585

[67] Kamalakkannan N, Prince PSM. Antidiabetic and anti-oxidant activity of Aegle marmelos extract in streptozotocin-induced diabetic rats. Pharmaceutical Biology. 2004;

[68] Ingle A. CPCSEA Inspections: Can it be done the AAALAC way? Journal of Laboratory Animal Science [Internet]. 2024 Dec 14 [cited 2025 Dec];3(1):31–4. Available from: https://doi.org/10.48165/jlas.2020.3.1.6

[69] Yadav M, Rana A. Aegle marmelos (L.): An underutilized plant with incredible pharmaceutical and nutritional potential. Food Chemistry Advances [Internet]. 2025 Feb 19 [cited 2026 May];6:100935. Available from: https://doi.org/10.1016/j.focha.2025.100935